COMPUTATIONAL FLUID DYNAMICS (CFD) ANALYSIS OF CAVITATION EFFECTS ON CENTRIFUGAL PUMP PERFORMANCE AND FLOW PATTERNS IN OIL AND GAS APPLICATIONS USING ANSYS SIMULATION TOOL

2023/2024 ACADEMIC SESSION
DEPARTMENT OF MECHANICAL ENGINEERING
UNIVERSITY OF BENIN

OKENE DANIEL OMONIGUHNO	**ENG1905639**
MADU CHUKWUEMEKA MIRACLE	**ENG1905630**
CHUKWUEZE BENJAMIN NWABUEZE	**ENG1905590**
IFORI SAMUEL EFEOGHENE	**ENG1905617**

SUPERVISED BY: DR. IKECHUKWU B. OWUNNA

CERTIFICATION

This is to certify that this research project titled: COMPUTATIONAL FLUID DYNAMICS (CFD) ANALYSIS OF CAVITATION EFFECTS ON CENTRIFUGAL PUMP PERFORMANCE AND FLOW PATTERNS IN OIL AND GAS APPLICATIONS USING ANSYS SIMULATION TOOL, was carried out under the supervision of Dr. Ikechukwu Bismark Owunna.

……. …….

Dr. Ikechukwu Bismark Owunna Date

Project Supervisor

……. …….

Engr. Martins Oshikueme Date

Project Coordinator 2023/2024

……. …….

Professor Godwin Ejuvwedia Sadjere Date

Head of Department

DEDICATION

We dedicate this report to God Almighty, whose grace has granted us the strength to accomplish all that was necessary for the success of this project. To our families, whose unwavering support and encouragement have been the foundation of our academic journey. To the Department of Mechanical Engineering, whose guidance and commitment to equipping us through extensive training and lectures have been pivotal in shaping us into who we are today. This work is also dedicated to all who have inspired and supported us along the way. Your faith in our potential has ignited our passion for learning and striving for excellence.

ACKNOWLEDGEMENT

We, as a group, extend our deepest gratitude, first and foremost, to God Almighty, the one who makes all things beautiful in His time. His grace, strength, and wisdom have been our guiding light throughout this project. We also express our heartfelt appreciation to our families for their unwavering support and understanding. Their words of wisdom and encouragement have been invaluable in helping us navigate the challenges of this journey.

Our sincere gratitude goes to our supervisor, **Dr. Ikechukwu B. Owunna**, whose unwavering support, insightful guidance, and words of encouragement have made this project both a learning experience and a rewarding endeavor. We are also grateful to the **Department of Mechanical Engineering, University of Benin**, for granting us the opportunity to undertake this project. Its commitment to academic excellence has provided us with a solid foundation for our work. Additionally, we appreciate the **Faculty of Engineering** for fostering an environment that nurtures learning and innovation. The knowledge and values instilled in us will remain invaluable beyond this project.

Lastly, we extend our sincere thanks to everyone who contributed to this project, whether directly or indirectly. In particular, we would like to acknowledge **Engr. Martins Oshikueme**, our project coordinator, for his invaluable guidance and support throughout this process.

ABSTRACT

The oil and gas industry relies heavily on centrifugal pumps to transport crude oil, yet cavitation remains a persistent challenge, reducing the lifespan and efficiency of pumps. Despite its significance in operation, crude oil cavitation has received limited attention, whereas existing studies have predominantly focused on water and other fluids. This study aims to fill this knowledge gap by developing a numerical approach to studying cavitation in crude oil centrifugal pumps. We used computational fluid dynamics (CFD) simulations with the ANSYS tool to investigate the complex flow patterns and cavitation phenomena in centrifugal pumps. In our work, we took a multi-faceted approach to capture the complexities of cavitation. We used a bubble model to track the nucleation, growth and implosion of vapor bubbles, a turbulent model to mimic the chaotic flow, and a multiphase model to account for the interactions between the crude oil in its liquid and vapor forms. The numerical approach is validated by comparing our results with the actual performance data of a pump from an established oil rig, yielding a margin of error of approximately 0.5%. The results highlight the significance of considering crude oil properties and pump design parameters to mitigate cavitation. Notably, the roughness value of the casing is found to have an acute impact on cavitation with even slight changes leading to increased cavitation activity. Furthermore, the backflow of crude oil is identified as a key factor that prompts discharge cavitation, emphasizing the need for careful design and operation of centrifugal pumps in the oil and gas industry.

TABLE OF CONTENT

LIST OF FIGURES

LIST OF TABLES

ABBREVATIONS AND KEYWORDS

CFD	Computational Fluid Dynamics
DNS	Direct Numerical Simulation
LES	Large Eddy Simulation
NPSH	Net Positive Suction Head
NPSHa	Net Positive Suction Head available
NPSHr	Net Positive Suction Head required
RNG	Re- Normalization Group
S-S	Schnerr-Sauer
VOF	Volume of Fluid
AD	Anno Domini
BC	Before Christ
BCE	Before the Common Era
CAE	Computer Aided Engineering
CVP	Concrete Volute Pump
DCM-RNG	Discontinuous Cavitation Model-Re-Normalization Group
FFT	Fast Fourier Transform
PDPs	Positive Displacement Pumps
SST	Shear Stress Transport
ZGB	Zwart-Gerber-Belamri
RANS	Reynolds-Averaged Navier-Stokes

CHAPTER 1

INTRODUCTION

1.0 Background of the Study

A pump is a device used to move liquids or slurries by mechanical action, typically converting electrical energy into hydraulic energy (Ravikumar, 2023) constitute essential mechanical apparatus crucial for the transportation of fluids, encompassing liquids and gasses, in diverse industrial, commercial, and residential settings. These mechanisms elevate the pressure of fluids, allowing them to surmount resistance and travel through conduits or pipelines to their designated endpoints. Pumps play a vital role in various sectors like water management, oil and gas, chemical processing, power generation, and manufacturing. Their efficiency in transferring fluids reliably is pivotal for numerous indispensable processes in contemporary society.

The predominant type, centrifugal pumps which are widely considered the most promising technological solution for future commercial endeavors (Kang et al., 2018), operate by transforming rotational kinetic energy into hydrodynamic energy. Fluid is admitted into the pump impeller axially and propelled outward by centrifugal force. This operational method is preferred due to its simplicity, effectiveness, and capability to manage substantial flow volumes. Centrifugal pumps find extensive application in the oil and gas industry owing to their durability and suitability for handling viscous fluids (C. Li et al., 2023a) or situations necessitating precise flow regulation. These pumps are critical for tasks that demand high pressure and precision, such as chemical metering, hydraulic systems, and fuel delivery.

Cavitation, a noteworthy phenomenon that can have a profound impact on the performance and durability of pumps, is the formation of vapour cavities in a liquid i.e. small liquid-free zones (“bubbles” or “void”) that are the consequence of forces acting upon the liquid (Mousmoulis et al., 2017a). It arises when the static pressure within the pump descends below the vapor pressure of the fluid (Orlandi et al., 2023a), resulting in the creation of vapor bubbles. These bubbles implode vigorously as they migrate to areas of higher pressure in the pump, producing strong shock waves. This sequence of events can lead to diverse unfavorable outcomes, jeopardizing both the effectiveness and structural soundness of the pump.

Cavitation inception studied by (Orlandi et al., 2023a) is easily understood considering cavitation number and the net positive suction head (NPSH). According to (Mousmoulis et al., 2017a) cavitation occurs as a result of implosion of bubbles arising from a situation where the net positive suction head available (NPSHa) falls below the net positive suction head required (NPSHr).

One of the primary repercussions of cavitation is the reduction in efficiency. The existence of vapor bubbles disrupts the seamless flow of fluid through the pump, generating a disorder and complex vortex distribution, thereby influencing the lift and drag forces of the system (Yan et al., 2021a; Liu et al., 2020). This interruption necessitates greater energy consumption (Shi et al., 2021) to sustain the desired flow rates, consequently diminishing the overall operational efficiency. The turbulent flow also contributes to escalated deterioration of pump components and the fluctuation of pressure of the pump (Che et al., 2019; Qiu et al., 2023a), further compromising performance as time progresses.

Furthermore, cavitation has the potential to inflict substantial harm on pump components. The forceful collapse of vapor bubbles subjects the surfaces of impeller blades, casing walls, and shafts to high-pressure shock waves. This recurrent impact induces erosion, pitting, and surface deterioration, all of which can undermine the mechanical robustness of the pump. Over time, these consequences can culminate in the catastrophic malfunction of crucial components, mandating frequent maintenance and replacement.

Aside from physical impairment, cavitation frequently manifests as identifiable noise and vibration (C. Li et al., 2023a). The swift implosion of bubbles generates a distinctive popping or knocking sound, serving as an early warning sign of cavitation within the pump. Concurrently, the uneven forces generated by bubble collapse can trigger mechanical vibrations, intensifying the wear on bearings and other mobile parts. Failure to promptly address these vibrations can result in structural fatigue and breakdown.

In the context of the oil and gas industry, the significance of cavitation extends beyond equipment damage. Cavitation can disrupt the flow of crude oil, leading to interruptions in production and transportation (C. Li et al., 2023a), which in turn impacts the profitability of operations. Given the strategic importance of oil and gas resources, especially in nations like Nigeria, where crude oil constitutes a major portion of the economy, addressing cavitation-

related challenges in pumps is paramount. For instance, the properties of crude oil—such as its high viscosity, non-Newtonian behavior, and the presence of impurities—make it more susceptible to cavitation compared to simpler fluids like water. The transport of crude oil through long pipelines and pumping stations in regions with fluctuating environmental and operational conditions adds further complexity to the problem (C. Li et al., 2023a).

As the global demand for energy grows and the reliance on oil remains strong, there is a need to optimize every aspect of crude oil transportation systems, particularly the pumping mechanisms. Pumps that fail due to cavitation can lead to costly repairs, downtime, and environmental hazards like spills. Therefore, understanding the dynamics of cavitation when crude oil is the working fluid, and finding solutions to mitigate its effects, is critical for improving pump reliability and operational efficiency.

This study seeks to explore these issues by employing Computational Fluid Dynamics (CFD) to analyze cavitation behavior in centrifugal pumps. Using CFD, it is possible to simulate the flow conditions within the pump, predict where cavitation might occur, and evaluate its effects on pump performance. The results of this study will provide insights that can help in the design and operation of pumps to minimize cavitation risks, especially under the challenging conditions typical of crude oil transportation systems in Nigerian oilfields and similar environments.

1.1 Statement of Problem

Cavitation is a well-known phenomenon in fluid systems, and substantial research has been undertaken into its effects in pumps that handle water and other relatively simple fluids. However, there is a significant gap in the literature when examining cavitation in pumps that handle crude oil (C. Li et al., 2023a). The properties of crude oil present unique challenges that are not fully addressed by existing studies (Luo et al., 2022a). Crude oil's high viscosity, varying densities, and the presence of impurities such as wax, sulfur, and water make its behavior in pumps significantly different from that of water. These factors increase the likelihood of cavitation, especially in the harsh operating conditions typical of oilfields.

The occurrence of cavitation in crude oil pumps can have serious effects. Beyond the immediate damage to the pump, cavitation can lead to flow instabilities, decreased efficiency, and operational downtime. In an industry where time is money, even minor disruptions can

result in significant financial losses. Moreover, in the context of Nigerian oilfields, where the infrastructure may be exposed to harsh environmental conditions and where operational efficiency is paramount, cavitation presents a serious challenge to reliable pump operation. Existing research has mostly focused on cavitation in pumps using water or other standard fluids, with only a few studies addressing more complex fluids like crude oil. This poses a knowledge gap that this study aims to fill. Specifically, the problem lies in the lack of comprehensive understanding of how the specific properties of crude oil contribute to cavitation in centrifugal pumps and how this phenomenon can be mitigated through design and operational adjustments.

Furthermore, while computational fluid dynamics (CFD) has been widely utilized to simulate cavitation in a variety of fluids, its application to crude oil systems is limited. There is a need for thorough CFD simulations that can forecast cavitation initiation, growth, and collapse in crude oil pumps, taking into account the fluid's specific features. This study will employ CFD techniques to simulate the flow of crude oil through a centrifugal pump and discover the essential elements influencing cavitation behavior. The project intends to provide practical solutions to the problem of cavitation in crude oil pumps, thus improving pump reliability and efficiency.

1.2 Objectives of the Study

The primary aim of this study is to employ Computational Fluid Dynamics (CFD) to model and examine cavitation in centrifugal pumps utilizing crude oil as the working fluid. The study aims to provide insights into the mechanisms of cavitation in such pumps and propose strategies to minimize its occurrence and adverse effects.

The specific objectives of the study are:

1. To simulate cavitation in a centrifugal pump handling crude oil using CFD techniques, focusing on identifying regions where cavitation is likely to occur.
2. To analyze the influence of crude oil properties (viscosity, density, and impurities) on cavitation dynamics, examining how these properties affect the formation, growth, and collapse of cavitation bubbles.

3. To study the effects of operating conditions (such as flow rate, pump speed, and suction head) on cavitation, determining the critical thresholds at which cavitation becomes severe.
4. To propose design and operational modifications that can reduce the occurrence of cavitation in crude oil pumps, thus improving pump performance and reliability.

1.3 Significance of the Study

Research into the exploration of the effect of cavitation on pumps performance is a critical area of study with wide-reaching benefits. These benefits extend on both the economical lifespan of pumps in oil and gas industry and its systems.

Some of the significance of this study include:

1. Improved Understanding of Cavitation in Crude Oil Pumps: The study addresses a significant gap in cavitation research by focusing on crude oil as the working fluid, as opposed to most cavitation studies that focus on water and other simpler fluids. This advances our understanding of how crude oil's distinct features (high viscosity, non-Newtonian behavior, and contaminants) influence cavitation.

2. Improvements to Pump Design and Performance

i. The study aims to optimize pump designs and operating conditions to reduce cavitation, resulting in more efficient and dependable crude oil handling in the oil and gas sector.
ii. Understanding cavitation behavior in crude oil systems can reduce equipment damage and associated risks.

3. Practical Application in Oil and Gas Industry

i. Relevance to Industry: The findings have direct industrial applications, particularly in improving the performance of pumps in Nigerian oilfields and other similar environments. The study can help operators reduce operational downtime caused by cavitation, enhancing productivity.
ii. Cost Savings: By minimizing cavitation-related issues, the industry can save on repair and replacement costs, while improving the overall efficiency of crude oil transportation systems.

4. Contribution to Computational Fluid Dynamics (CFD) Research: The study contributes to the application of advanced CFD models, such as the VOF multiphase model and the S-S

bubble model, specifically for cavitation analysis in crude oil systems. This can be leveraged by future researchers working on complex fluids in similar engineering applications.

1.4 Scope of the Study

This study focuses on centrifugal pumps, which are the most commonly used pump type for crude oil transportation in the oil and gas sector (C. Li et al., 2023a). The specific pump geometry and design will be modeled using SolidWorks, ANSYS SpaceClaim and Design Modeler to ensure that the findings are applicable to real-world pump designs used in the industry. The working fluid for this study is crude oil, with its unique properties (such as viscosity, density, and impurities) being central to the research. Different grades of crude oil have varying properties, and this study will focus on a typical grade of crude oil found in Nigerian oilfields.

This study will employ Computational Fluid Dynamics (CFD) techniques to simulate cavitation in crude oil pumps. Specifically using the Volume of Fluid (VOF) multiphase model to track the formation and collapse of cavitation bubbles, while the Schnerr-Sauer (S-S) bubble model will be applied to simulate the growth and dynamics of individual bubbles. These models will allow for a detailed analysis of how cavitation develops in crude oil pumps under different operating conditions. The study will simulate cavitation under a range of operating conditions typical of Nigerian oilfields. These conditions include different flow rates, pump speeds, and suction head values. By varying these parameters in the simulations, the study will identify the critical thresholds at which cavitation becomes severe and propose strategies to mitigate it.

1.5 Methodology

Computational Fluid Dynamics (CFD) Technique:

This study employs a simulation-based approach using computational fluid dynamics (CFD) to analyze the effects of cavitation on pump performance. CFD is a powerful tool that allows for detailed visualization and analysis of fluid flow patterns, pressure distributions, and cavitation phenomena within the pump.

The simulations began with steady-state analysis to understand average flow characteristics and identify potential cavitation zones. This initial approach is less computationally intensive and provides a foundational understanding of flow patterns. Based on the steady-state results,

transient simulations were selectively performed on smaller portions of the geometry and shorter time frames to capture time-dependent behaviors without overloading the computational resources.

The mesh resolution was set to a moderate density, with finer mesh elements in regions prone to cavitation (e.g., near the impeller) and coarser mesh in less critical areas. This resulted in a total cell count that was kept manageable - under one million cells. The k-ε turbulence model was utilized for its balance of accuracy and computational efficiency, and the Schnerr-Sauer cavitation model was selected for its robustness and common use in engineering applications.

Boundary conditions included a uniform inlet velocity and a fixed outlet pressure, with no-slip conditions applied on all solid boundaries. Simplifications such as assuming incompressible flow and maintaining isothermal conditions were made to reduce computational requirements. Minor geometric features that do not significantly affect the flow were also ignored to streamline the simulation process.

In terms of geometry and mesh, the pump geometry was simplified to focus on key components such as the semi-open impeller and volute casing. ANSYS Meshing was used to create structured mesh in critical areas and unstructured mesh elsewhere, targeting a total cell count of around 500,000 to 1,000,000 cells.

The simulation settings in ANSYS Fluent included using a pressure-based solver, steady-state analysis initially. The Viscous Model was set to k-ε (RNG), and the Multiphase Model to Volume of Fluid (VOF) with Schnerr-Sauer cavitation. Solution methods included the SIMPLE scheme for pressure-velocity coupling and second-order upwind for spatial discretization to ensure better accuracy.

For initialization, standard initialization from the inlet was used, and a few hundred iterations were run for steady-state convergence. If transient simulation was needed, a small time-step based on the Courant number (e.g., 0.001 seconds) was chosen, limiting the number of time steps to a few hundred to a thousand to keep the computational load manageable.
By following this methodology, the study aims to provide a comprehensive analysis of cavitation effects in centrifugal pumps with semi-open impellers, balancing accuracy with computational feasibility.

1.6 Limitations

In this study, several limitations were acknowledged due to computational and resource constraints:

1. **Mesh Resolution and Accuracy:** Due to the constraint of a maximum of one-million mesh element imposed by the ANSYS Student License, the mesh resolution was optimized to balance computational feasibility with the need for accuracy. A moderate mesh density was used, with finer elements in regions where cavitation is expected (e.g., near the impeller) and coarser elements in less critical areas. This approach may result in less accurate predictions of cavitation zones and flow details in highly localized regions.

2. **Turbulence Modeling:** The standard k-ε turbulence model was chosen for its balance between computational efficiency and accuracy. However, this model may not fully capture all turbulence characteristics, especially in highly turbulent or complex flow regions. More advanced models like LES (Large Eddy Simulation) or DNS (Direct Numerical Simulation) were not utilized due to their higher computational demands.

3. **Cavitation Model Assumptions:** The Schnerr-Sauer cavitation model was employed, which assumes a homogeneous mixture of vapor and liquid phases. This simplification might overlook some complexities of cavitation bubble formation and collapse dynamics, potentially affecting the accuracy of cavitation predictions.

4. **Physical Assumptions:**
   i. Isothermal Conditions: The simulations were conducted under isothermal conditions, neglecting any thermal effects that could influence cavitation and fluid properties.
   ii. Idealized Boundary Conditions: Uniform inlet velocity and fixed outlet pressure were used to simplify the problem setup. In real-world scenarios, these conditions can be more complex and variable, potentially impacting the simulation results.

5. **Data Limitations:** The input data for the simulations were based on standard pump models and manufacturer specifications. While these provide a reasonable basis for the study, they may not reflect the specific conditions encountered in all industrial applications. Variations in pump design, operating conditions, and fluid properties could affect the generalizability of the findings.

CHAPTER 2

LITERATURE REVIEW

2.0 Historical Development of Pump Technology

For centuries, the evolution of pumps and pumping systems which is keyed on improving its efficiency, has been a pivot for driving the advancements in engineering and industries where the need of pressurizing or moving a fluid from one location to another finds use. The evolution of the pumping system emerged as a need of moving water from one location to another where transportation of water, based on gravitational pull was not applicable.

The first pumping system was called a "shadoof". It was invented around 2000 BC in Mesopotamia, during the time of Sargon of Akkad (around the 24th and 23rd centuries BCE). This pumping system was used to lift water from a river into an irrigation field and consisted of a long, tapering, nearly horizontal wooden pole, mounted like a seesaw (Stavros, Gerasimos, Nicolaos, Wang Li, Mohammad, Aldo, and Andreas, 2015). This pumping system was capable of lifting a small amount of water and required the use of large animal force, making it relatively inefficient.

Figure 2.1: Shadoof – The first pumping system

The waterwheel, a revolutionary pumping system, was invented by the Romans around 650 BC (Source: of technology in the classical world Oxford: Oxford University Press, 2000 Oleson, John P.). This radical device consisted of a wheel with blades and was used to discharge a large amount of water, though the wheel was to be turned manually. The waterwheel's design was later refined by the Greeks, who added a horizontal axle and improved the blade design (Source: Promising approaches to this process are: A. John W. Humphrey, Greek and Roman Technology)

Figure 2.2: The Water Wheel (Tympanon)

Thus, the “tympanon” pumping system was created in the process of striving for higher water output per a single rotation. The tympanon featured a compartmentalized body, but was still limited by the static head (Source: Skelton R.W. “The History of Pumps”) Meanwhile, in ancient China, the Jiégāo (Chinese water wheel) was invented during the Han Dynasty (206 BC - 220 AD), featuring a similar design to the Roman waterwheel (Source: Taking into consideration more specifically, the article focuses on the inventions that were made by the ancient Chinese people (the title of the article is ‘Ancient Chinese Inventions’ by Deng Yinke). The Chinese Jiégāo was widely utilised for irrigation and water supply, with enhancements implemented during the Tang Dynasty (618-907 AD) (Source: "The Cambridge History of

China, Vol. 3" by Denis Twitchett). The design of Jiégão was subsequently embraced by Arab engineers, who then introduced it to the Middle East and Europe during the Islamic Golden Age (Source: "The History of Science in the Islamic World" by Howard R. Turner).

In 250 BC, the hydraulic endless screw of Archimedes also called "Archimedean Screw" was invented (Mike Hurlbatt, 2016). This pumping system is made of a helical array of blades wrapped around a central cylinder and supported within a fixed trough with a small gap that allows the screw to rotate freely (Arash and William, 2021). Essentially, It is a large screw, open at both ends and encased lengthwise in a watertight covering. When one end of the screw is placed in water and the screw is elevated at an angle and then turned, water trapped in the air pockets between the threads rises from the open lower end, up the length of the screw, and is released through the upper open end.

Figure 2.3: The Archimedean Screw Pump

This device has the advantage of being simple to construct and also transporting water containing muds, sand or gravel but also has a low static head and a low efficiency.

During the Hellenistic period, Ctesibius (Greek:Κτησίβιος; fl. 285–222 BC) is credited with inventing the Force Pump in around the 3rd century BC. He established the principles of compressed air and its use in pumpage, and is fondly referred to as the ‘Father of Pneumatics’. Ctesibius’ Force Pump theory (circa 250 BC) proposed the possibility to design a device which could use pressure of air and water to create a water jet or to raise water from wells (Ctesibius, 250 BC). This design makes it appropriate for uses like irrigation, fire extinguishers, and water supplies. But it is lower than modern pumps, because leakages, friction, and pressure losses affect this kind of pump.

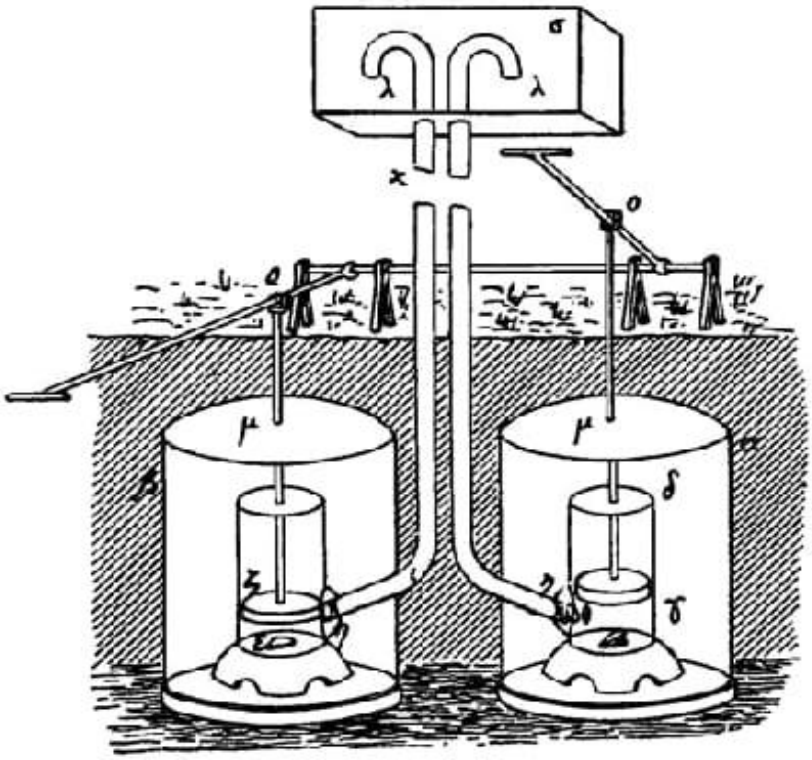

Figure 2.4: The Force Pump

After the fall of the great Roman Empire, pump technology became stagnant for nearly fifteen centuries (Williams, 2019). It was only during the Enlightenment Period (circa 1685–1815) that hydraulic science began to be focused on again. It was during this era that pumps had a rebirth, and over the next couple of centuries, new ideas and inventions began to flood the market, all of which led to the design of modern-day pumps.

In the year 1619, a Frenchman, Grollier de Servière, N. (1596-1689), charted the early designs for a gear pump, which laid the foundation for later innovations in fluid transfer technology (Servière, 1619). Serviere's design involved a pair of interlocking gears that rotated to displace fluid, setting the stage for the development of more complex gear pumps in the centuries to

come. Over the next several decades, inventors and engineers built upon Serviere's concept, refining the design and materials to create more efficient and reliable gear pumps (Johnson, 2020).

It was around this time that Johannes Kepler (MLA: Kepler, Johannes. (1604). Gear Pump) proposed his idea of the Gear Pump (Kepler, 1604). Kepler's design involved two circular gears with teeth that meshed together, a central shaft that connected the gears, a chamber that surrounded the gears, creating a sealed space, and inlet and outlet ports for fluid flow (Kepler, 1604). Later, in 1636, a German engineer named Pappenheim (Pappenheim, A. (1636). Double, deep-toothed rotary gear pump. Leipzig: VEB Verlag) built upon Kepler's work and invented the double, deep-toothed rotary gear pump (Pappenheim, 1636).

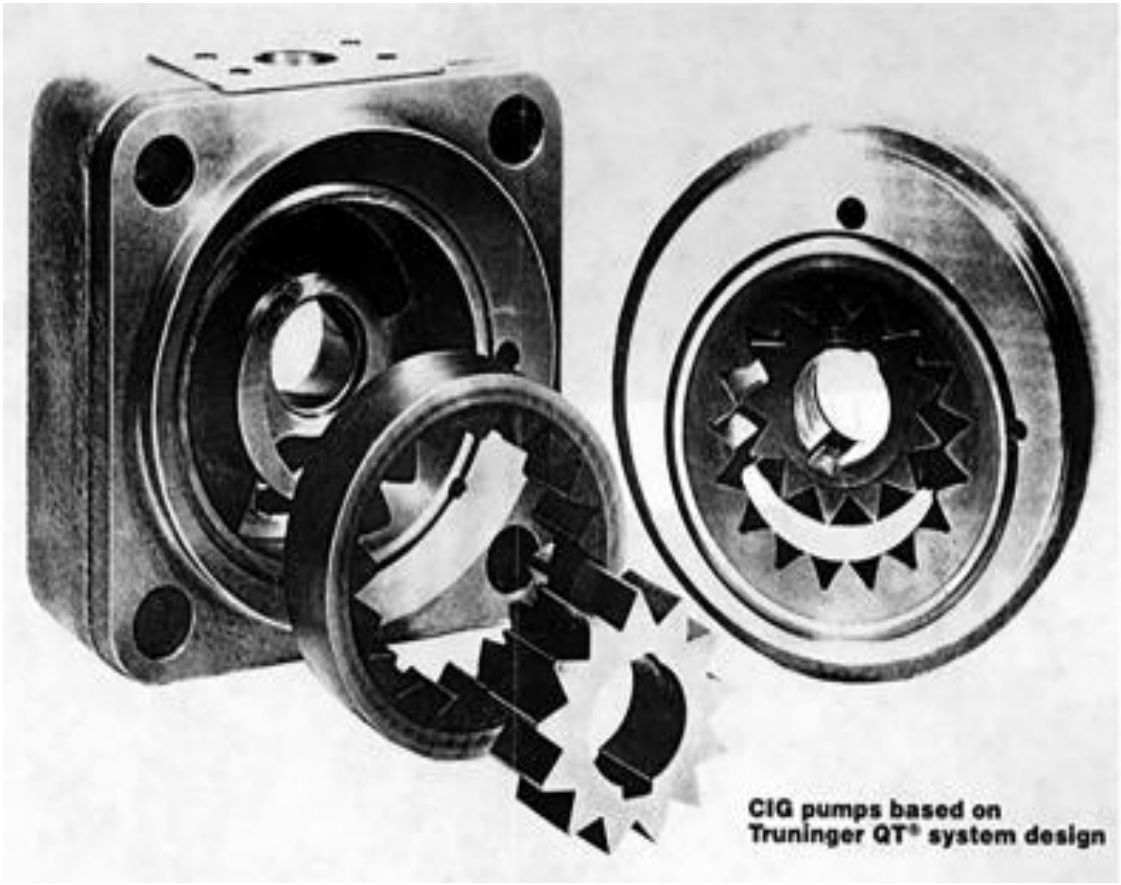

Figure 2.5: Kepler's Gear Pump

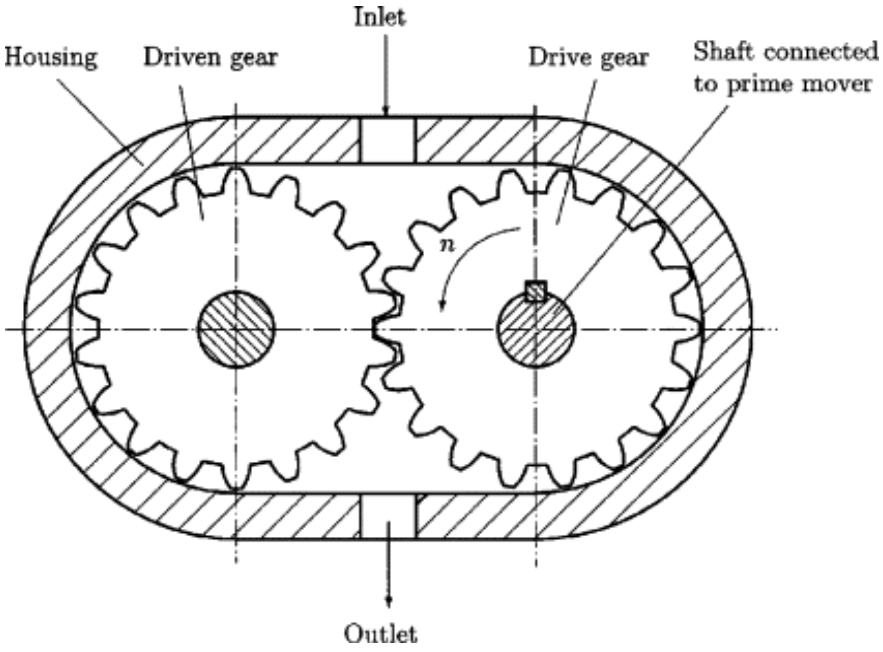

Figure 2.6:Schematic of Kepler's Gear Pump

In the year 1650, Otto van Guericke introduced the piston vacuum pump to the world and became an important pioneer in the progress of pump technology. The pump design was a piston and cylinder, through the piston down move, a vacuum chamber was formed through the control of several valves.

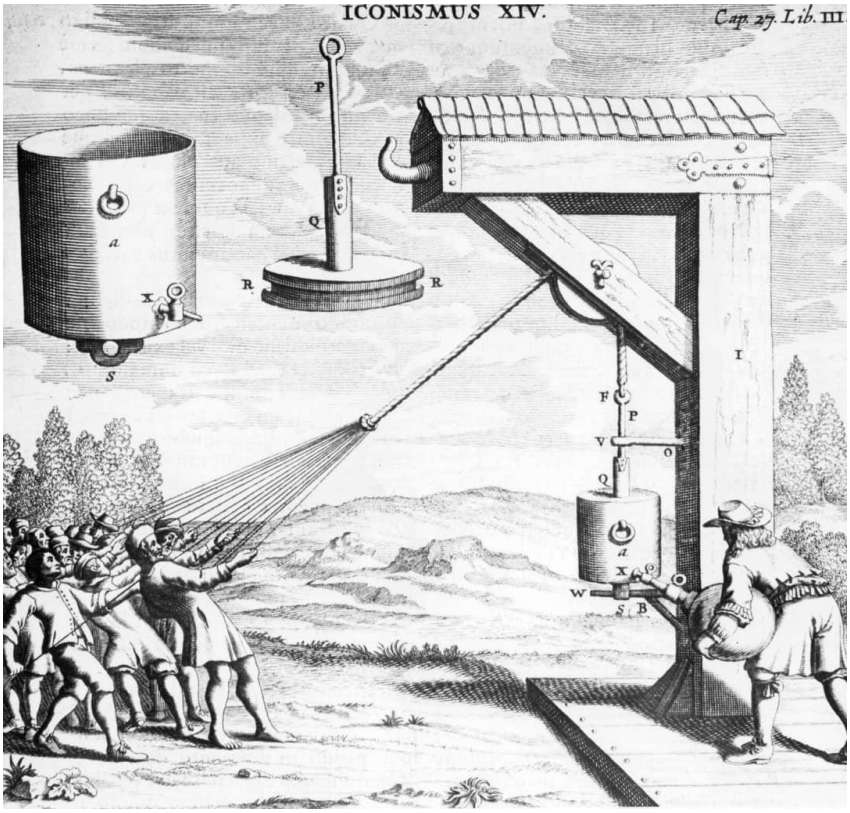

Figure 2.7: Guericke's piston vacuum pump

This experiment involved a vacuum pump where Guericke proved how powerful his vacuum pump was by sealing the two halves of the Magdeburg Hemispheres and then removing all the air from the chamber. This work not only showed how a mechanical pump could be used to create a vacuum but also paved the way to the further improvement of the efficiency of vacuum pumps in the future by providing ideas for the improvements in design. It cannot be questioned that Guericke significantly contributed to pump development, and subsequent inventors Denis Papin and Thomas Newcomen, based on his findings, advanced their ideas on the use of vacuum pumps and steam engines.

Towards the end of the 17th century specifically in 1675, Sir Samuel Moreland (1625-1695), an English Engineer and inventor patented an improved form of packed plunger water pump. The first ever design had a cylindrical chamber with a plunger that went up and down; this cycle produced suction and pressure. The plunger was smartly slipped with a leather or rope packing that assisted to enhance the efficiency of the plunger together with improving the seal difference.

Another improvement Moreland's design brought to the fore is the sensible increase in the efficiency and reliability of the pumping process. Therefore, the packed plunger pump was applied in many fields such as water supply and disposal, drainage, and irrigation.

Centrifugal pump is firmly credited by historians to have been invented by Denis Papin in 1687. Apparently, the idea of centrifugal force had existed prior to Papin, yet no prior developer had created a machine that solely relied on the force; despite early prototypes being built with the use of this force, Papin created and constructed the first genuine centrifugal pump as we understand it now (Papin, 1687). They include: His machine had an inlet chamber where the water or air flows in, then a spinning impeller that spun the water or air in a whirlpool that raised its pressure as well as flow rate. This design led to the development of the modern centrifugal pumps that encompass several applications in diverse fields such as water supply systems, industries and in electricity generation.

Centrifugal pumps can be traced back as far as the late 17th century while their design was not efficient until the 1840s (Thompson, 2019). According to Reti again, the idea of a subordinate centrifugal pump like device was the first ever conceived by Italian Renaissance engineer, Francesco di Giorgio Martini in 1475 (Reti, 1963). And it was only in 1851 when British

inventor John Appold introduced what are called curved vanes, a component that dramatically improved the performance of the pump (Appold, 1851). Appold's design improved upon providing the centrifugal pump the ability to provide higher pressures and volume rates, making them useful across a wide number of industrial and commercial uses (Appold, 1851).

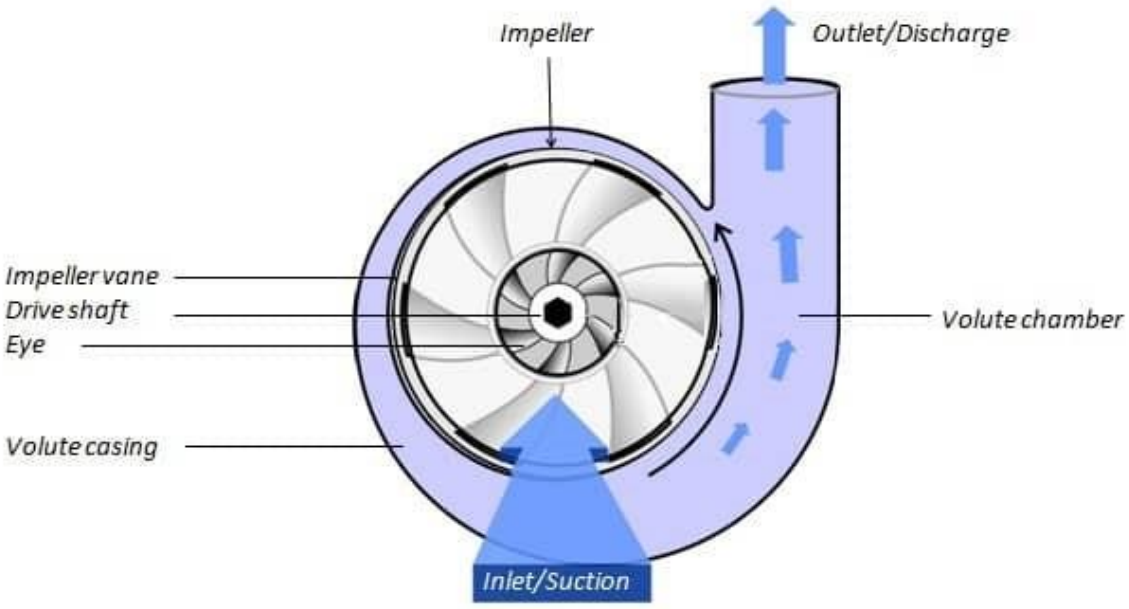

Figure 2.8: Centrifugal Pump

The year 1738 can be considered as one of the most significant in the development of industrial machinery. It was the year when the Ural hydraulic machinery plant was built and, for the first time in the world, equipped with the automated pump machinery.

It was also in this year that Bernoulli introduced his principle that describes the relationship between velocity, density and pressure. In fluid dynamics, Bernoulli's principle states that for an inviscid flow, an increase in the speed of the fluid occurs simultaneously with a decrease in pressure or a decrease in the fluid's potential energy. The principle is applied to various types of fluid flow and is loosely known as Bernoulli's equation.

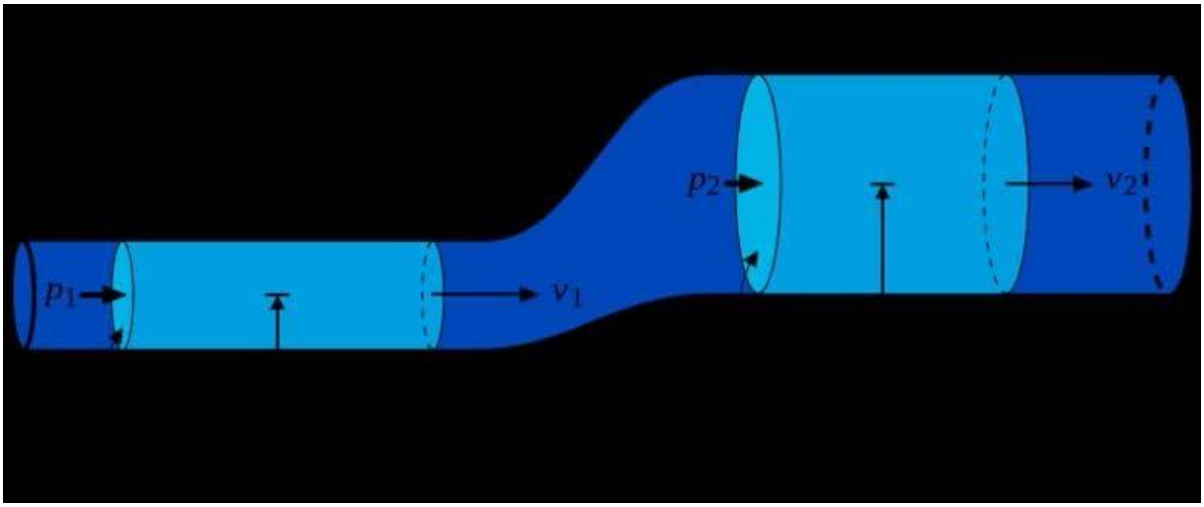

Figure 2.9: Bernoulli's Principle

In 1782, James Watt, a Scottish inventor, who worked on the steam engine's connecting rod crank mechanism that enabled converting reciprocating motion into rotary motion, develops an oscillating piston machine with a wing-shaped rotary blade that opens inlet ports in an enclosure created by a curved radial wall that divides the chamber nearly in half.

The year 1790 saw Thomas Simpson deploy steam power to pumping engines in the context of municipal water uses. Simpson's work brought about the establishment of Simpson and Thompson Co, which later transpired to Worthington Simpson. From the information provided by Graces Guide, Simpson played a central role in steam pumping engines. He provided apparatus for diverse waterworks undertakings within London and the other areas.

In 1830, Revillion improved pump technology by coming up with the modern screw pump where a right-handed screw and a left-handed screw meshed and rotated in an opposite direction to transport fluids most effectively.

Henry R. Worthington, an American Mechanical Engineer, invented the first direct-acting steam pumping engine in the year 1840. Worthington Pump designed its first products to power canal boats and U.S. naval vessels. Worthington later pioneered pump designs for boiler feed, oil pipeline and hydro-electric applications.

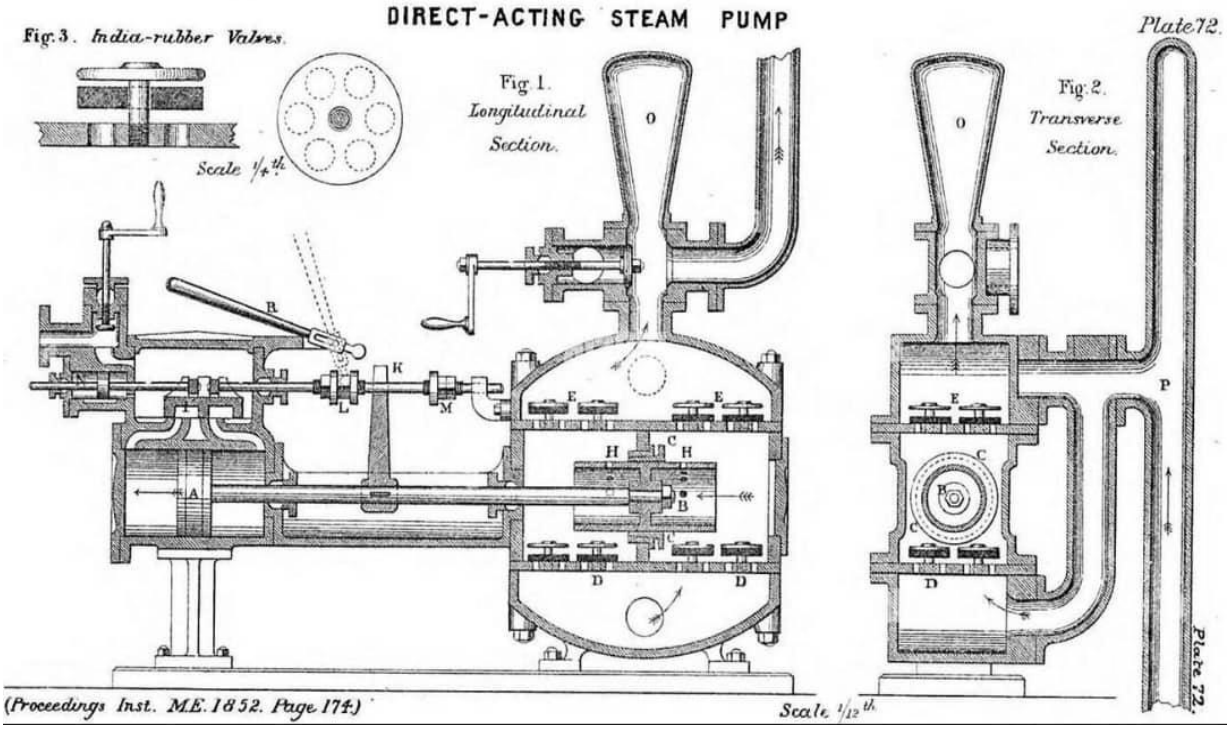

Figure 2.10: First direct acting steam pump

The first wooden pump banded with iron was produced in 1848 by Goulds in Seneca Falls, New York around the time that gold mining took off in California. He believed that an iron pump would eliminate all the limitations of the wooden pump. It would be strong and efficient and provide flowing fresh water to users.

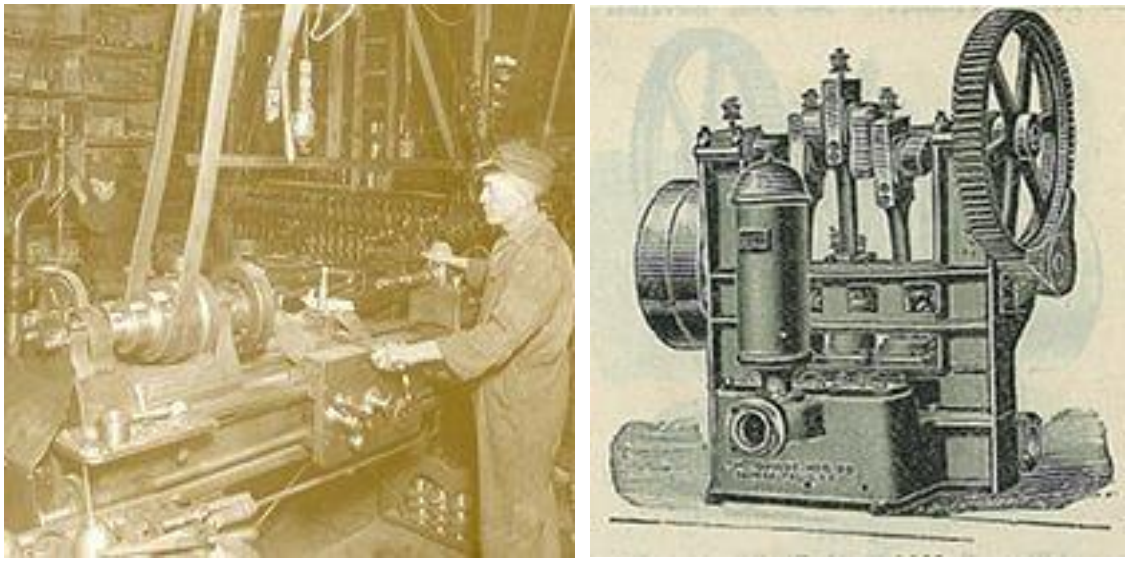

Figure 2.11: Wooden pump banded with Iron by Goulds

Developed in 1855 by J. Pease, the Mnemosyne pump (Diaphragm Pump) was based on the mammal heart and could be considered as one of the first cases of biomimetics in engineering.

The pump itself resembles the heart's diaphragm – septum which divides the right and left atrium of the heart, thus making sure that the blood pumping mechanism in the human body is effective as well as independent. This biomimetic strategy returned the Mnemosyne pump to a constant flow, similar to the blood circulation in a heart, which makes the Mnemosyne pump be considered one of the unique examples of following nature.

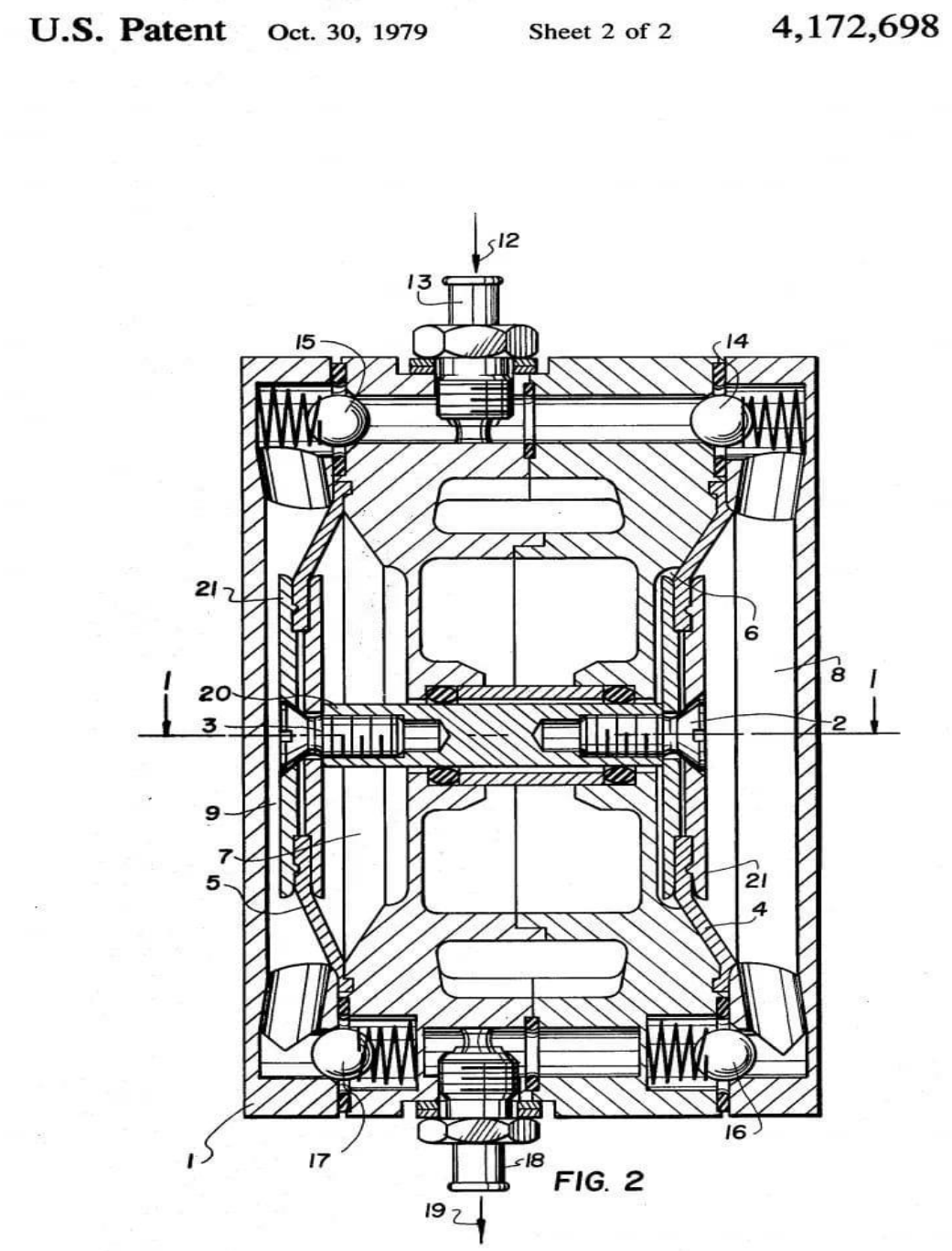

Figure 2.12: US patent for J. Pease, the Mnemosyne pump (Diaphragm Pump)

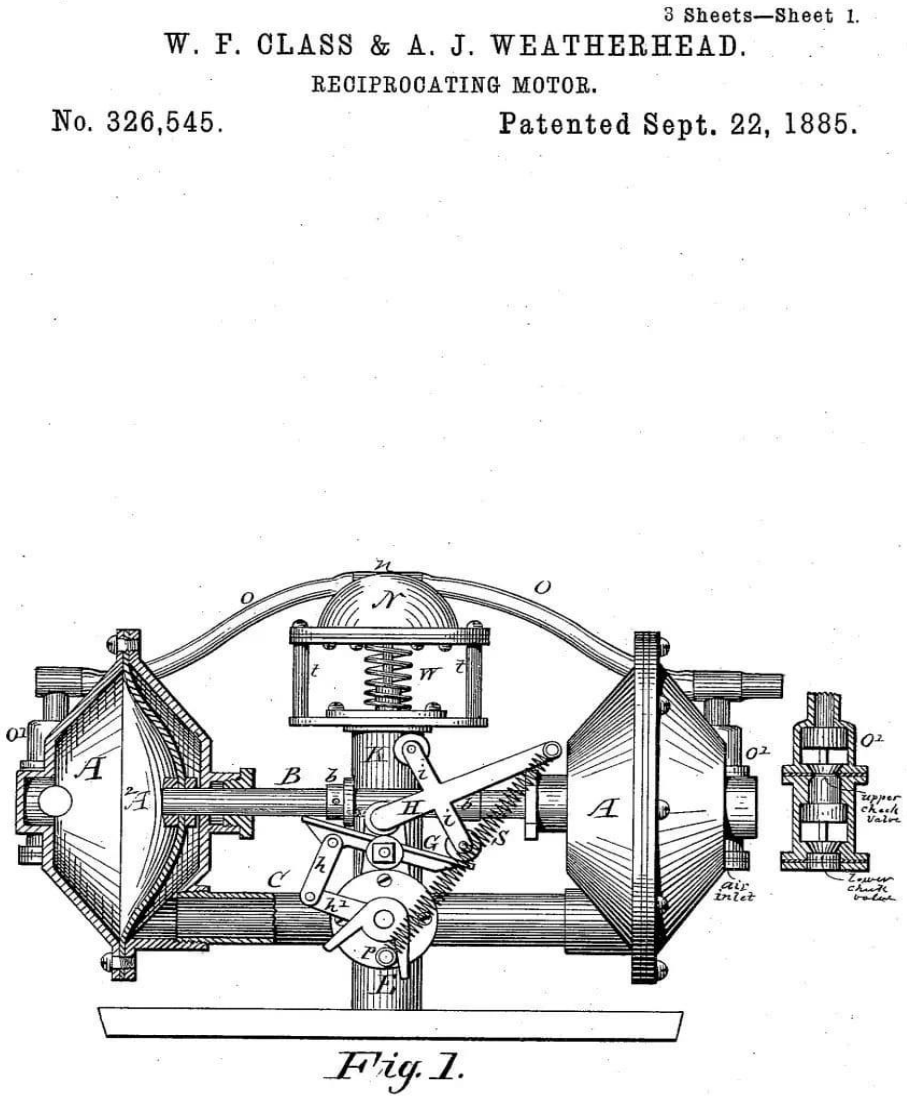

Figure 2.13: US patent for Class and Weatherhead Reciprocating Pump

It was in 1857 that Worthington developed the horizontal, duplex, direct-acting steam pump for boiler feed. This novel design had two steam cylinders, the small and the large, which meant that it was possible to use steam at a different pressure. While the small cylinder operated at the boiler pressure, the exhaust steam was pulled through a receiver and delivered to the larger cylinder at low pressure. It was also a direct-acting mechanism that secured effective transmission of steam energy that favoured both the suction and the discharge strokes hence efficiency. In Worthington's design, the pressure difference of the two cylinders was adopted and thus became the technology in steam pumps replacing the old models of steam pumps for feeding boilers and this further solidified his position as a pioneer in pump science and manufacture.

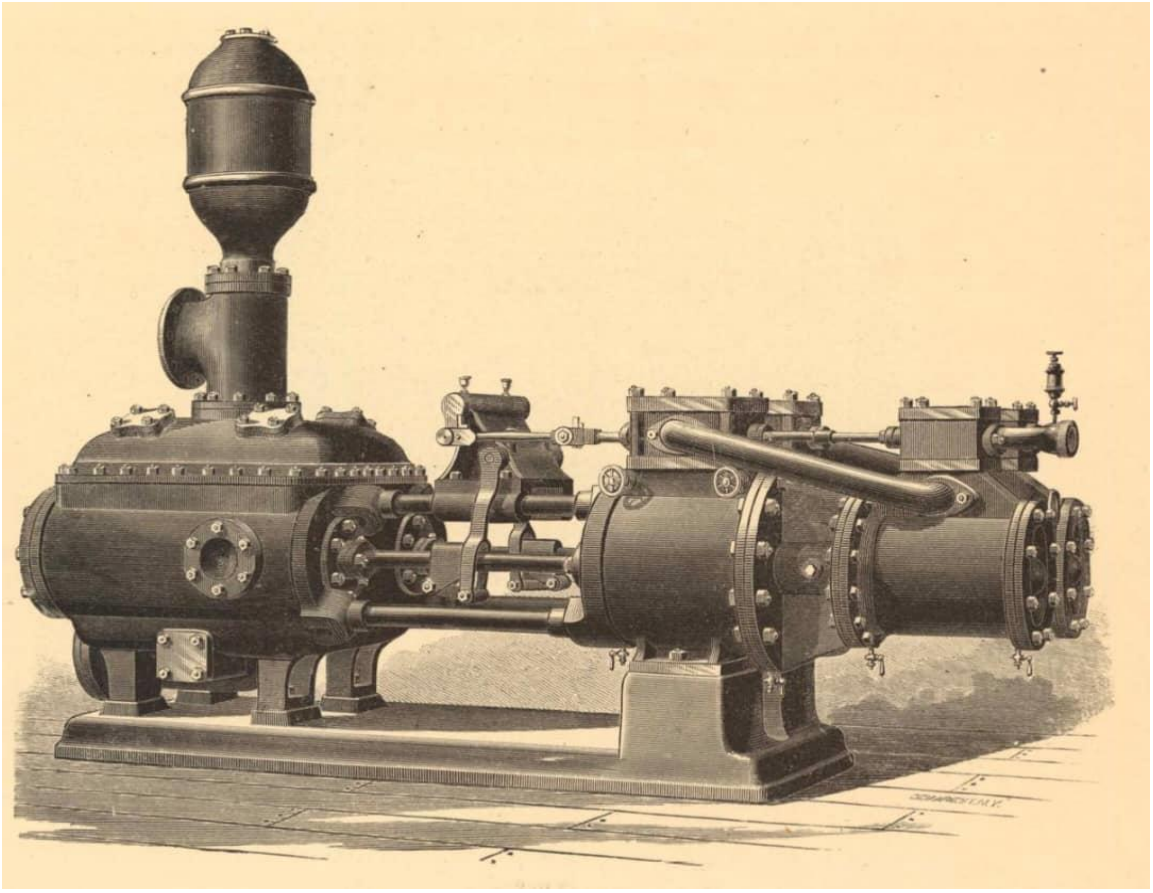

Figure 2.14: Worthington's horizontal, duplex, direct acting steam pump

In 1860, Adam Cameron established the Cameron Steam Pump Works and became a leading figure in reciprocating steam pump engines' evolution. His inventions were used in the engines of merchant marine and United States naval ships. Cameron's pumps evolved over the years and were applied to water resources, oil pipeline and refining as well as boiler feed.

Louis Bergeron invented the Concrete Volute Pump (CVP) in 1917 in France during the world war to solve the problem of steel scarcity for pumps. This type of pump is very efficient, reliable and can easily be maintained which made it to be used in energy and drainage. Most importantly, all the 58 units of French Nuclear Power Plant units as well as many Nuclear Power Plants in China, Korea and South Africa have selected CVPs condenser cooling water pumps because of the manufacturer's ability to handle high flow rates at low total head rise, which naturally makes CVPs ideal for large scale industrial applications (R Prunières et al, 2012)

2.1 History of Cavitation

Cavitation, which is a multiphase flow phenomenon, is the formation of vapour cavities in a liquid –i.e. small liquid-free zones ("bubbles" or "voids") – that are the consequence of forces acting upon the liquid (Prakash, Ajinkya, 2014).This phenomenon although was first conjectured by L. Euler in his theory of water turbines and was first mentioned in his paper "Théorie plus complette des machines qui sont mises en Théorie plus complette des machines qui sont mises en" (A more complete theory of machines that are set in motion by reaction with water) in 1754, and also in the publication of a solution to the problem of the dynamics of the collapse of a spherical cavity in a fluid by William Henry Besant, which had been presented by the Anglo-Irish mathematician George Stokes, in 1859, the effect cavitation was first discovered and studied by Barnaby and Parsons in 1893. Their investigation into cavitation arose during the analysis of performance problems in British warships, HMS Daring - The warship was meant to reach a speed of 27 kn but it only attained a speed of 24 kn before failing - in 1885 (Shengcai Li, Christopher, Yoichiro, 2015). Due to their observation during the course of their study of the cause of the failure of the warship, they suggested that this failure was due to the damaged propeller blade which occurred as a result of implosion of water vapour bubbles. Barnaby also suggested that the HMS Daring had a given boundary for a particular propeller speed, or a given maximum tensile strength of the water, at which a breakdown of the propeller inflow occurs. This tensile strength corresponds to thrust per projected screw area of 11 ¼ lbs/inch² in case of the “Daring”, as Thornycroft proposed.

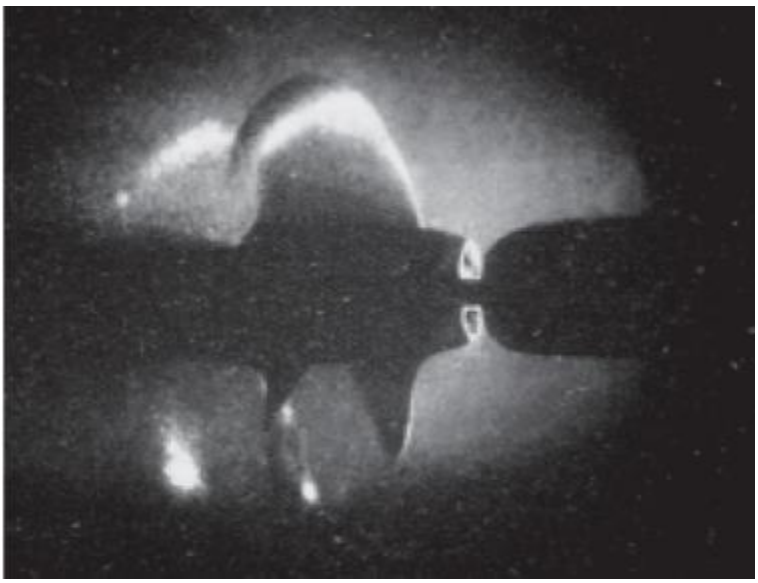

Figure 2.15: One of the first propeller cavitation photographs from Parsons first tunnel (1895)

This phenomenon was later coined "cavitation" derived from the Latin word “cavus,-a, -um”(Engl. “hollow”) by R. E. Froude in 1895, which was proven true by Parson during his initial trial designing a high power boat “turbinia” (This HMS Turbinia was designed for a top speed well over 30 kts but disappointedly failed at a speed below 20 kts) in 1895 (Alhelfi, Sunden, 2014).The HMS Turbinia was designed by Parson in order to demonstrate the application of the compound steam turbine in marine propulsion (Arndt, Pennings, Bosschers, Terwisga, 2015). This approach used by Parson in solving cavitation problems set a stage for the techniques used in modern research.

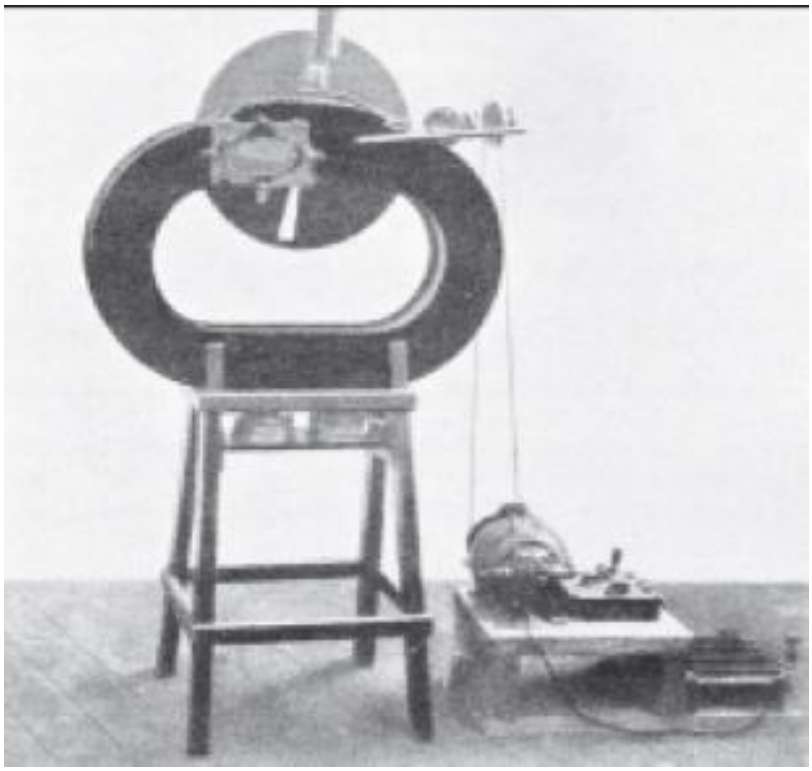

Figure 2.16: Parsons first cavitation tunnel (1895)

Parson also devised a water version of a venturi-type wind tunnel with a special stroboscope in order to study this phenomenon and during his studies using this mechanism, he discovered the relationship between cavitation and the damage caused on the propeller of a British warship. Parsons' early works were first focused on the phenomenon in connection with “the racing of the screw and loss in propulsion effect” until in 1910 when his works were focused on “the effects of cavitation in another form, namely erosion and pitting of the blades”.

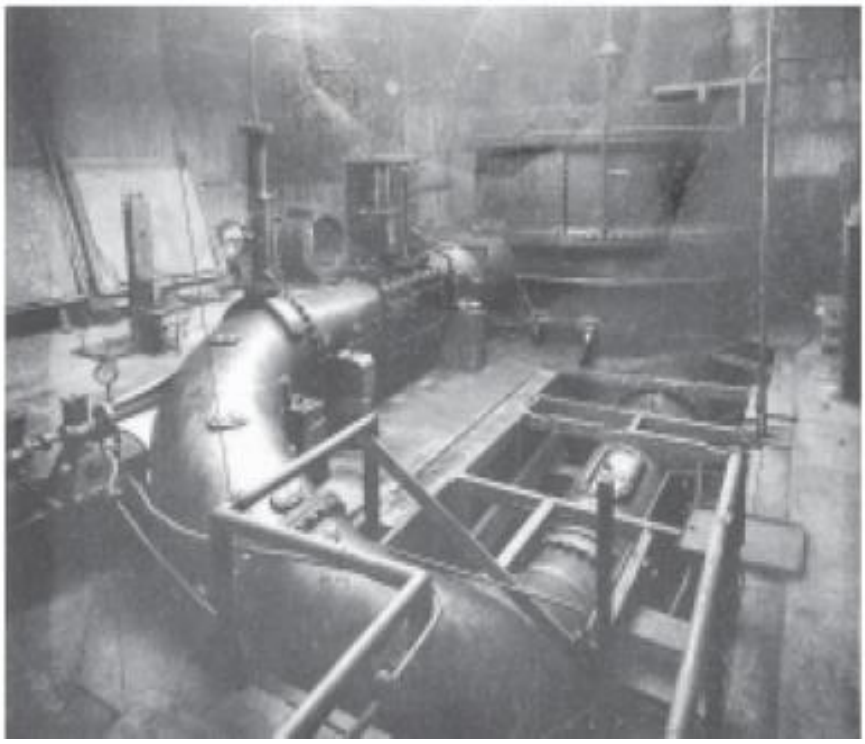

Figure 2.17: Parsons larger cavitation tunnel (1910)

Although the investigation of this phenomenon increased drastically during the years, the physics of this phenomenon was not fully established until in 1917 when Lord Rayleigh laid the theoretical foundation for cavitation study by solving the problem of the collapse of an empty cavity in a large mass of liquid. The Rayleigh derived equation was named as "**Rayleigh–Plesset equation**" or "**Besant–Rayleigh–Plesset equation**". This equation, which was derived using the solution of Besant, is a nonlinear ordinary differential equation which governs the dynamics of a spherical bubble in an infinite body of incompressible fluid.

Rayleigh–Plesset equation which describes the motion of the bubble surface was later investigated by Neppiras. Neppiras on his investigation stated that Rayleigh–Plesset equation accurately describes the motion of the cavity-surface over a limited number of cycles for all types of stable cavitation, and also for transients where the bubble surface velocity never exceeds about 1/5 of the velocity of sound", but under violent transient conditions the bubble surface velocity may approach, or exceed, the velocity of sound (Alhelfi, Sunden,2014).

In 1930, Ackeret investigated the effects of cavitation in high-speed flows. This experiment was carried out using a test Venturi nozzle, a pressure measurement tool. During the

experiment, pressure measurements on five different profiles on circular arcs and aerofoils were investigated.

Ackeret in 1930 showed that for cavitating conditions, there is a linear proportionality between on one hand the difference of static head minus vapour pressure and on the other the dynamic head of the inflow. These observations lead to the result that cavitation inception in a liquid occurs when the pressure at a given point of the flow compared to a given pressure reaches the saturated water vapour pressure belonging to the given fluid temperature (Nikolett, Balázs, Rajmund, 2019).

Minnaert in 1933 also set the stage for understanding the acoustics of cavitation and gas filled bubbles which was published in the paper "On Musical Air Bubbles and the Sounds of Running Water". Minnaert studies which were basically on bubble resonance in fluids and cavitation focused on how bubbles behave and emit sound when they oscillate and collapse (Long, Mourad, 2024). The detrimental effect of cavitation and the need to mitigate the effect of cavitation grew more in the oil and gas sector with the evolution of centrifugal pumps. In 1972, John S. Knapp, James W. Daily, and Frank G. Hammitt investigated the effect of cavitation in large centrifugal pumps and turbines which are critical for oil refineries and petrochemical plants. During their investigation, the concept of cavitation inception bubble dynamics was studied, focusing on effects of nuclei size and surface roughness on cavitation inception. In 1994, Sato and Okamura conducted critical work on cavitation in multiphase pumps, which was focused on the study of the complex interaction of different fluids and how cavitation impacted pump performance.

In 2015, Schilling and colleagues investigated the cavitation in high-pressure water pumps used for hydraulic fracturing (fracking) operations. This investigation established a more suitable method of optimizing the designs of pumps used for fracking operations. In 2017, Arana and Anzola in their journal "Cavitation and Hydraulic Systems" investigated the impact of cavitation in mud pumps and other drilling equipment used in offshore oil platforms. During their investigation, the effects of cavitation on safety in extreme environments were highlighted. With the advancement in computer aided engineering (CAE) over the years, the study of the impact of cavitation, ways of designing pumps to mitigate this effect of cavitation has been improved drastically.

2.2 Effects of Cavitation

Cavitation, a classic gas–liquid two-phase flow phenomenon has greatly affected the overall performance of mechanical systems. This phenomenon which has been studied by various researchers has been observed to be the leading factor for the failure of many machineries just like the HMS Daring and Numerous studies have investigated the effects and factors that contribute to cavitation in centrifugal pumps, including pump design, operating conditions, and fluid properties.

Cavitation inception in centrifugal pumps which is established when the net positive head available (NPSHa) falls below the net positive head required (NPSHr) i.e when the net positive head is below the vapour pressure of the fluid. This phenomenon causes a large loss in the internal energy of the fluid, significantly destabilizing the internal flow field and correspondingly degrading the hydraulic performance. Cui and Li investigated internal flow characteristic of energy loss in high-speed centrifugal pumps by employing the SST k-ε turbulence model and the results obtained at the course of their investigations revealed that the energy loss in the impeller reduced as the axial distance between the inducer and impeller increased (Liu, Xinyang, Zuchao, Yongcao,Guangwu, Chuancang, Luo, 2024).

.

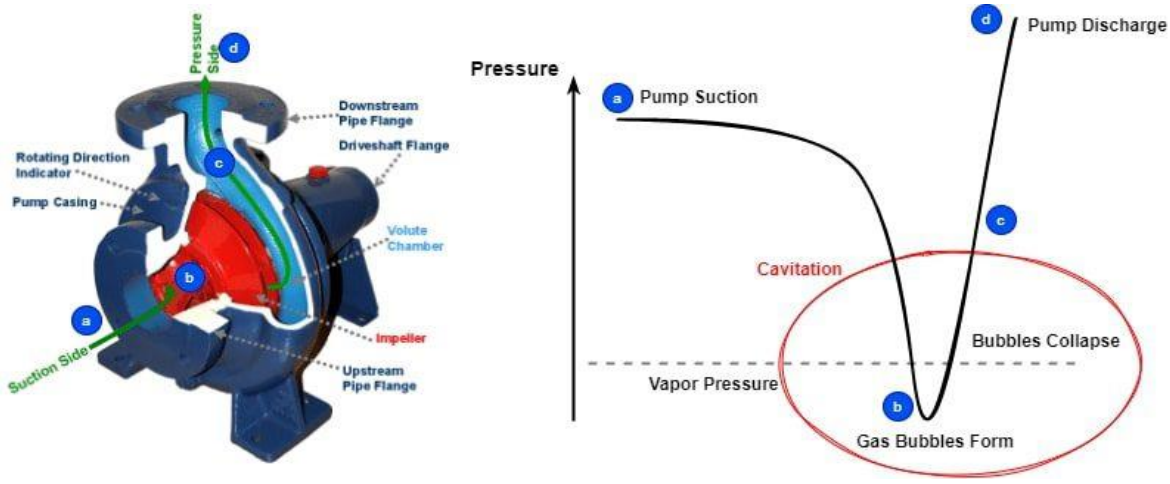

Figure 2.18: Pressure profile through centrifugal pump undergoing cavitation

Cavitation also causes erosion of both the impeller and the casing. The erosion of the centrifugal pump is as a result of the shockwave which is released during the implosion of the bubbles. The shockwave causes pitting on the surface of the impeller blades and on the casing. Zhu (2021) in his investigation of "cavitation erosion on Centrifugal Pump Blades by the

DCM-RNG Method" showed that the erodible area predicted is in the middle and downstream of the blade and that there is a small erodible area at the entrance of the blade.

Cavitation also creates large noise, which is as a result of the release of ultrasonic frequencies due to the rapid implosion of vapour bubbles. The research program at NEL (National Engineering Laboratory) on cavitation showed the noise characteristics of typical centrifugal pumps which was studied using noise measurements on a series of pumps of different sizes running at various speeds (P. J. McNulty, I. S. Pearsall, 1982).

Wang et al. also investigated the noise produced in centrifugal pumps and he also studied the occurrence of cavitation at the inlet of the centrifugal pump impeller. Upon his studies, he obtained the relationship between the cavitation distribution in the impeller and the vibration and noise characteristics of the pump.

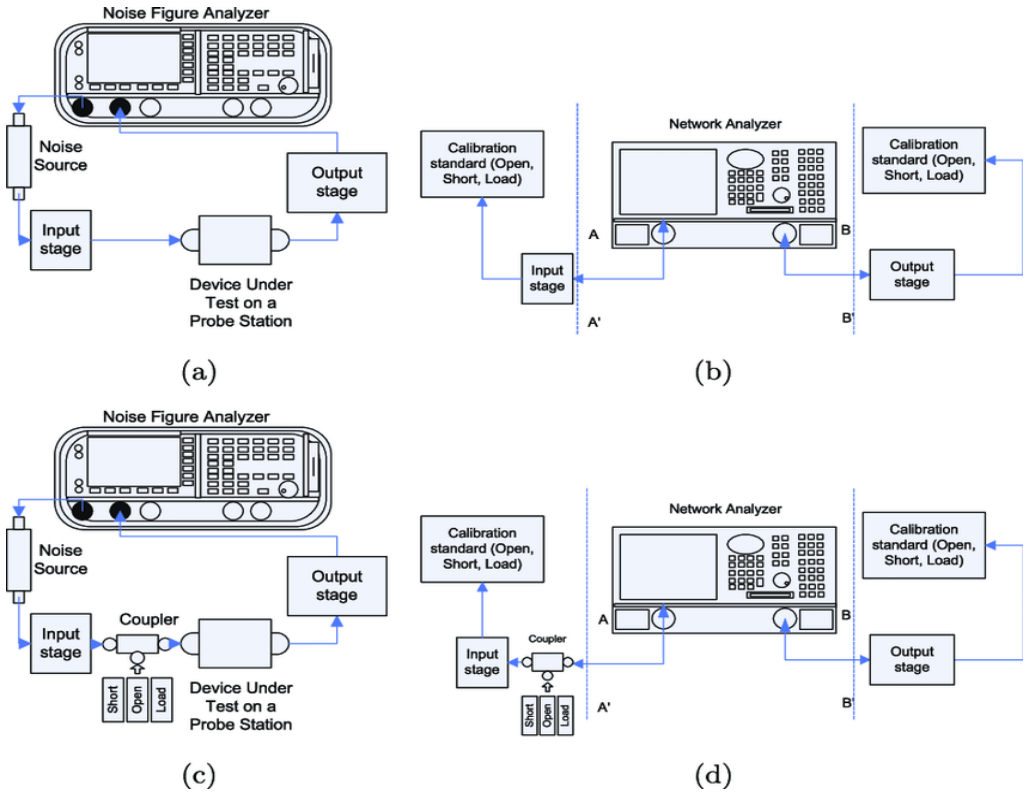

Figure 2.19: Noise Instrumentation Setup

Cavitation also causes large vibration of the centrifugal pump and the entire system. Zargar (2014) analysed the effect of cavitation on centrifugal pumps related oil industry for cooling circulation water system by studying the vibration signal in time waveform and frequency domain using FFT method (Fast Fourier Transform), which he found that the vibration signals

increased suddenly under cavitation condition, drastically reducing the performance of the pump (Al-obaidi, 2019). Furthermore, cavitation can also result in the formation of vapour pockets and cavities, which can alter the flow dynamics within the pump and lead to decreased performance (Zhu et al., 2023).

Cavitation is not limited to centrifugal pumps, but also occurs in other types of pumps that operate under similar principles. For instance, Archimedes screw pumps, which are commonly used for irrigation and water supply, are also susceptible to cavitation (Thornycroft, 1895). Positive displacement pumps (PDPs), such as gear pumps and lobe pumps, can experience cavitation depending on the effective mechanical separation of the suction and discharge regions. This separation, which is necessary for the volumetric efficiency of the pumps, is realised by means of a mechanical contact point after the mating of the gear's teeth (Francesco, Luca, Massimo, 2023).

Additionally, cavitation has been observed in rotary pumps, such as vane pumps and screw pumps, particularly at high speeds and low pressures (Zhang, 2019). The effects of cavitation on pump performance and efficiency are similar across these pump types, leading to reduced flow rates, increased energy consumption, and damage to the pump and its components (Binama, 2022).

(Hu et al), in his study of cavitation in centrifugal pumps, analyzing the occurrence of cavitation in an overloaded condition using the ZGB model reported that at overloaded conditions, flow separation characterized by unsteady vortex shedding from the tongue, causes the low-pressure zone near the tongue. (Hu, Q.a , Yang, Y.a , Cao, W, 2020). (Corvaglia et al), while studying the effect of cavitation, evaluated the impact of tooth space pressure in case of incomplete filling which he reported a fall in the flow rate when a lower pressure value was reached (Corvaglia, Rundo, Casoli, Lettini, 2021).

Cavitation reduces the overall efficiency of all pumps in operation (Centrifugal pumps and other types of pumps e.g. gear pumps, vane pumps etc. performs poorly under cavitation conditions). Ali Abdul (2014) computational investigation on the effect of cavitation on centrifugal pumps outlines that the percentage efficiency drop of the pump is greater than 3% and that the cavitation regions appear at the leading edge of suction side of the impeller blades

which represents the lowest pressure area inside the computational domain of the centrifugal pump

2.3 Recent Advances in Cavitation Erosion Reduction in Centrifugal Pumps

“Cavitation can reduce the efficiency and service life of centrifugal pumps, and a long-term operation under cavitation conditions will cause cavitation damage on the surface of material” (H. Zhu et al, 2021). This review focuses on the findings of recent research on cavitation, with reference to the mechanisms of onset, the different approaches to modelling the phenomenon and minimizing its impact on pump design and functionality.

Research conducted by Anil Kumar Yadav and Prof. Shamir Daniel (2022) concerns the application of micro-grooved impellers in the decrease of cavitation and the increase of centrifugal pump efficiency. Using CFD, they surveyed smooth and grooved impellers, thereby proving that the grooved impeller is more efficient and less cavitated. In this research, significant failure modes related to centrifugal pumps used widely in water supply and sewerage industries were found out. In the presented results, the possibilities of microgeometry modifications in impeller design to reduce losses and improve the pump's operation have been shown.

Khan & Zhao Weiguo (2024) studied reduction of cavitation in centrifugal pumps with curvilinear barriers on the blade. These numerical findings showed a substantial decrease in the increase rate of cavitation volume, the stream structure improvement and a reduction of the vortex force. By creating high pressure waves to collapse cavities and the alteration of transition characteristics of flow, curvilinear barriers provide a feasible active control cavitation suppressing technique. This novel practice has important connotations to the design and practice of centrifugal pumps especially in the oil and gas industry where the menace of cavitation induced injury and loss of capability is out of proportion. The work presented here offers some indication for enhancing the efficiency, reliability, and durability of the pump system and indicates that there is great potential for additional exploration of curvilinear barrier systems.

In their study, Luo et al. (2022) examined vibration characteristics of nuclear centrifugal pumps especially when at Low flow rates. Through ANSYS CFD simulation and experimental

analysis on a HAZ50-250 prototype, they discussed reverse flow and rotating stall phenomena. Effects indicated that the vibration frequencies were within a range of 0.23-0.25 times the rotational frequency due to higher blade sensitivity to hydraulic oscillations. Other harmonics were also detected which included the vibration frequencies at the rotation frequency and two times the rotation frequency. The study showed the origin of hydraulic vibration and some recommendations for the optimization of this phenomenon's effects; the information is beneficial for vibration and pump design assessments.

M. Burak Samsul (2021) looked into the possibility of using the blade cup method in reducing cavitation on marine propellers. In this paper, Samsul made a numerical and comparative study of cavitation of a no-cup cavitating propeller and cupped one. The result showed that it is possible to reduce cavitation by using the blade cup method and thus enhance the durability of the propeller components. More significantly, the researchers found variations in the thrust, torque and efficiency of the cupped propeller. In this sense, this research is useful in advancing more effective and long-lasting marine propulsion systems.

In this context, this study proposes to use the ANSYS simulation tool to study the impact of cavitation on centrifugal pump performance and efficiency with the ultimate goals of establishing the critical design parameters and operating conditions which will guard against cavitation and consequent degradation of pump performance, with the ultimate view of improving efficiency, reliability and durability of these pumps. Our study aims at filling the gaps in the existing literature concerning cavitation in centrifugal pumps as well as, offering the relevant information for the improvement of the centrifugal pumps systems.

CHAPTER 3

METHODOLOGY

3.0 Governing Principles and Models for Cavitation Analysis

3.0.1 Theories of Fluid Flow

For this study, the methodology incorporates foundational theories of fluid flow to analyze cavitation effects in centrifugal pumps. Fluid flow theories, including infinitesimal region equations, and Navier-Stokes equation, describes fluid behavior under varying pressure and velocity conditions. These principles which are also the backbone of computational modelling enables the accurate prediction of flow patterns and identification of cavitation-prone regions.

Infinitesimal Control Volume Equations

In analyzing fluid motion, two approaches are often utilized, the control volume (finite region) and the infinitesimal region approach. The control volume approach makes use of integral equation to reveal the basic dimensionless parameters that govern fluid motion, while the infinitesimal region approach make use of differential equations and it serves as the bedrock of most computational fluid dynamics commercial software including ANSYS FLUENT- which was utilized in this study.

I. Conservation of Mass: The Continuity Equation

The Continuity Equation ensures that mass is conserved in a fluid flow system. For a control volume, this principle is expressed as:

$$\frac{\partial \rho}{\partial t} + \nabla \cdot (\rho \vec{U}) = 0 \ldots\ldots\ldots\ldots\ldots (3.0.1.1)$$

Where:

ρ is the fluid density (kg/m³),

$\vec{U}$ is the velocity vector (m/s),

t is time (s).

In the case of an incompressible fluid, such as crude oil under consideration, the density (ρ) remains constant, simplifying the equation to:

$$\nabla \cdot \vec{U} = 0 \ldots\ldots\ldots\ldots\ldots (3.0.1.2)$$

This equation implies that the net flow rate into any control volume (the centrifugal pump in this case) equals the net flow rate out. In cavitation analysis, the Continuity Equation helps track the flow distribution in the pump, particularly in regions where velocity changes might induce pressure drops, leading to vapor bubble formation.

II. Conservation of Momentum: The Navier-Stokes Equations

The Navier-Stokes equations describe the motion of fluid particles by applying Newton's second law to a fluid element. For an incompressible, Newtonian fluid like crude oil, the equations take the form:

$$\rho(\frac{\partial \vec{U}}{\partial t} + \vec{U} \cdot \nabla \vec{U}) = -\nabla p + \mu \nabla^2 \vec{U} + f \ldots\ldots\ldots\ldots\ldots (3.0.1.3)$$

Where:

p is the pressure (Pa),

μ is the dynamic viscosity (Pa·s),

f represents body forces (e.g., gravity).

The term $-\nabla p$ accounts for pressure gradients, while $\mu \nabla^2 \vec{U}$ represents viscous stresses. These equations enable detailed analysis of the flow fields in the pump and are essential for understanding the pressure and velocity distribution – a very important data for understanding cavitation occurrence. Solving the equation above numerically with appropriate boundary conditions captures when local pressure drops below the vapor pressure of crude oil, thus the formation of bubbles and ultimately the cavitation effect.

III. Conservation of Energy: The Energy Equation

The Energy Equation accounts for energy transformations within a fluid system. In differential form, for incompressible flows, it is expressed as:

$$\frac{\partial}{\partial t}(\frac{\rho \vec{U}^{\,2}}{2} + \rho e + \rho \Phi) + \nabla \cdot (\vec{U}\,(\frac{\rho v \vec{U}^{\,2}}{2} + \rho e + \rho \Phi + p) - \kappa \nabla T) = 0 \ldots\ldots (3.0.1.4)$$

Where:

e is the internal energy per unit mass,

Φ represents potential energy per unit mass,

κ is the thermal conductivity,

T is temperature (K).

In centrifugal pumps, this equation describes how mechanical energy (imparted by the impeller) is converted into kinetic and pressure energy. Regions of significant energy loss can contribute to cavitation onset.

3.0.2 Multiphase Flow Modeling: Volume of Fraction (VOF) Model

Multiphase modelling involves using computational techniques in simulating the behavior of systems involving more than one distinct phase. These phases which can be in states (e.g. solid, liquid or gas) and interacts which each other through mechanism like mass transfer, momentum transfer, phase transfer and energy transfer.

There are various types of multiphase models (e.g. Eulerian model, Mixture model, Inhomogeneous model, Volume of fraction model) but in this study, the volume of fraction (VOF) model is used.

Volume of fraction model is a surface-tracking technique designed to simulate immiscible multiphase flows. This model solves computational fluid dynamics of immiscible fluids by tracking the fraction of the cell boundary occupied by each phase using various transport equations.

VOF method uses a marker function which is represented by a fraction of computation grid cell occupied by the fluid to be the reference phase (liquid Crude-oil in this simulation). This model uses the volume-fraction/color fraction "C" to locate the transition and the fraction of a phase in a cell grid. This function which depends on the characteristics function "H" varies between the constant value one in full cell or zero in empty cell. The volume-fraction function "C" is defined as an average value of the characteristic function "H" ("C" is the discrete function of "H").

The volume-fraction of a phase is given by:

$$C = \frac{Volume\ of\ cell\ grid\ occupied\ by\ the\ phase}{Total\ volume\ of\ cell\ grid} \quad \ldots\ldots\ldots\ldots\ldots (3.0.2.1)$$

The volume-fraction with respect to the characteristic function is given as:

$$C = \frac{1}{\triangle V} \oint H(x, y, z, t) dV \quad \ldots\ldots\ldots\ldots\ldots\ldots (3.0.2.2)$$

Where: $H(x, y, z, t) \rightarrow Charateristic\ function,\ C \rightarrow Volume - fraction, \triangle V \rightarrow Volume\ of\ cell\ grid$

The characteristic function "H" tells us about what particular phase is present in the grid cell and is obtained using the equation below:

$$H(x,y,z,t) = \oint \delta(x-x')\delta(y-y')\delta(z-z')dV \ \ldots\ldots\ldots\ldots\ldots\ldots (3.0.2.3)$$

In order to accurately account for the motion of the fluid and change in interface at a given interval, VOF model uses the following transport equations:

I. Momentum Transport Equation

$$\frac{\partial(\rho\vec{U})}{\partial t} + \nabla\cdot\left(\rho\vec{U}\right) = -\nabla P + \nabla\cdot\left(\mu\left(\nabla\vec{U} + \nabla\vec{U}^{T}\right)\right) - F_s \ \ldots\ldots\ldots\ldots\ldots\ldots (3.0.2.4)$$

Where: $\rho \rightarrow Density$, $P \rightarrow Pressure$, $\mu \rightarrow Coefficient\ of\ viscosity$,

$\vec{U} \rightarrow Velocity\ profile$, $F_s \rightarrow Tension\ force$,

For multiphase simulation using VOF model, in order to account for the densities and coefficient of viscosity of the phase at the interfaces, VOF model compute the value of density and coefficient of viscosity needed in the momentum transport equation using the formula:

$$\{\rho,\mu\} = C\{\rho_1,\mu_1\} + (1-C)\{\rho_2,\mu_2\} \ldots\ldots\ldots\ldots\ldots\ldots (3.0.2.5)$$

Separating the density and coefficient of viscosity, this formula becomes:

$$\mu = C\mu_1 + (1-C)\mu_2 \ \ldots\ldots\ldots\ldots\ldots (3.0.2.6)$$

$$\rho = C\rho_1 + (1-C)\rho_2 \ \ldots\ldots\ldots\ldots\ldots\ldots\ldots (3.0.2.7)$$

Where: $\mu_1 \rightarrow Coefficient\ of\ viscosity\ of\ phase\ 1$,
$\mu_2 \rightarrow Coefficient\ of\ viscosity\ of\ phase\ 2$,
$\rho_2 \rightarrow Density\ of\ phase\ 2$, $\rho_1 \rightarrow Density\ of\ phase\ 1$
The tension force from equation is given by:

$$F_s = \delta K\hat{n}\delta_s \ \ldots\ldots\ldots\ldots\ldots\ldots (3.0.2.8)$$

Where: $\delta \rightarrow Surface\ tension$, $K \rightarrow Curvature$, $\hat{n} \rightarrow Unit\ normal$, $\delta_s \rightarrow Delta\ function$

From equation 3.0.2.8, "δ_s" is given by:

$$\delta_s = |\nabla C| \ldots\ldots\ldots\ldots\ldots\ldots (3.0.2.9)$$

The unit normal is obtained using the formula:

$$\hat{n} = \frac{\nabla C}{|\nabla C|} \ldots\ldots\ldots\ldots\ldots\ldots\ldots (3.0.2.10)$$

"K" from equation 3.0.2.8 describes the curvature of the interface. This value which is a function of the unit normal is given below:

$$K = \nabla \cdot \hat{n} \ldots\ldots\ldots\ldots\ldots\ldots\ldots (3.0.2.11)$$

Substituting equation 3.0.2.10 into equation 3.0.4.11,

$$K = \nabla \cdot \left(\frac{\nabla C}{|\nabla C|}\right) \ldots\ldots\ldots\ldots\ldots\ldots\ldots\ldots (3.0.2.12)$$

II. Volume Fraction Transport Equation

$$\frac{\partial C}{\partial t} + \nabla \cdot \left(C\vec{U}\right) + \nabla \cdot (C(1-C)\mu) = 0 \ldots\ldots\ldots\ldots\ldots\ldots\ldots\ldots\ldots (3.0.2.13)$$

During computation, the cell grid where interface exist and the volume fraction of each phase forming this at the cell grid changes with respect to time due to the dynamic motion of the phases. In order to account for this changes (interface reconstruction), VOF model using a tracking computation algorithm (this method involves computationally remeshing of the fluid domain using this algorithm e.g. geometric reconstruction).

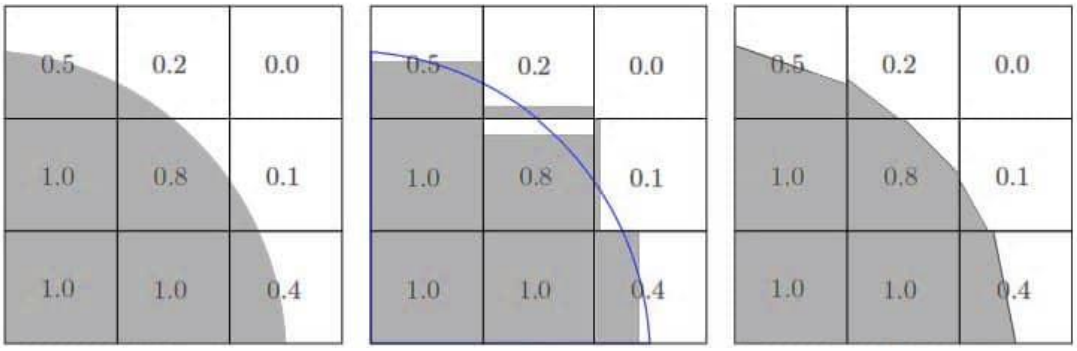

Figure 3.1: Volume fraction, PLIC, SLIC

During the simulation of a multiphase process, in order to prevent an interface from moving more than one cell grid per time step, preventing smearing or numerical diffusion (ensuring stability of the interface capturing algorithm), courant number is calculated. The courant number is given by the equation below:

$$Courant\ Number = \frac{|\vec{U}| \triangle t}{\triangle x} \ldots\ldots\ldots\ldots\ldots\ldots (3.0.2.14)$$

3.0.3 Cavitation Bubble Dynamics: Schnerr-Sauer Model

Cavitation simulation involves the formation, growing and the collapsing of bubbles. In order to track the growth and collapsing of bubbles in the simulation, computational fluid dynamic (CFD) solvers (Ansys fluent in our case) use various bubble transport equation e.g. Schnerr–Sauer, Zwart-Gerber-Belamri etc. depending on the set up. This bubble equations are derived from the generalized Rayleigh–Plesset equation, given as:

$$\frac{P_{vap}(t) - P_{\infty}(t)}{\rho_1} = R_b \frac{d^2 R_b}{dt^2} + \frac{3}{2}\left(\frac{dR_b}{dt}\right)^2 + \frac{4v_1}{R}\frac{dR_b}{dt} + \frac{2F}{\rho_1 R_b} \quad ------(3.0.3.1)$$

Where:

$\rho_1 \rightarrow Density\ of\ the\ surrounding\ flood, P_{vap} \rightarrow Pressure\ inside\ bubble$

$P_{\infty} \rightarrow External\ pressure\ infinitely\ far\ away\ from\ the\ bubble, R_b \rightarrow Bubble\ radius,$

$R \rightarrow Vapour\ generation\ or\ evaporation\ rate, v_1 \rightarrow Kinematic\ viscosity$

Although Rayleigh–Plesset equation helps in tracking the dynamic growing and collapsing of bubbles, it does not account for the viscosity, superficial tension and non-constant external pression contributions. Due to the difficult of applying Rayleigh-Plesset differential equation (3.0.3.1) into a multiphase flow model, it is simplified to the equation below.

$$\frac{dR_b}{dt} = \sqrt{\frac{2}{3}\frac{P_{vap}(t) - P_{\infty}(t)}{\rho_1}} \quad ------(3.0.3.2)$$

Equation (3.0.2.2) is sufficient to first estimate the phenomenon but has a drawback of an unrealistic development of the bubble due to the neglecting of the other terms.

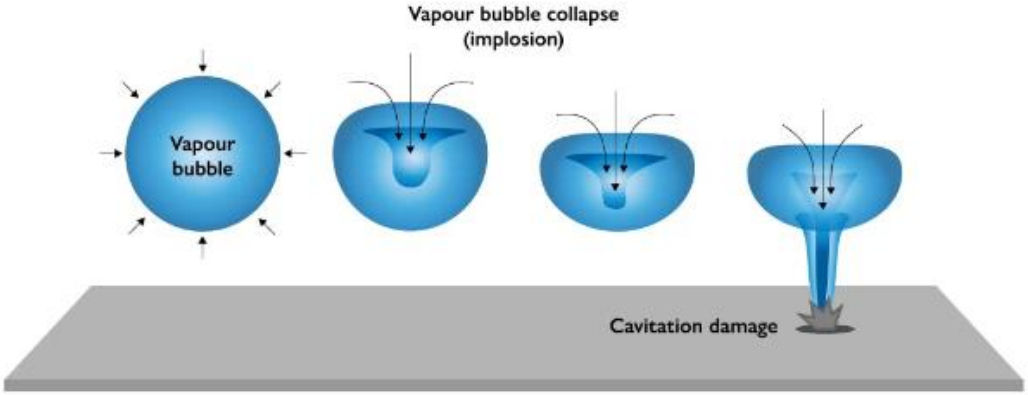

Figure 3.2: Formation, growth, and collapse of bubble

For the simulation of the phenomenon of cavitation formed during the transport of crude oil and in order to accurately track the formation, growth, collapse, and the volume occupied by the bubble, Schnerr-Sauer cavitation model is used as the bubble transport equation.
The Schnerr-Sauer cavitation model is given by:

$$R\frac{d^2R}{dt^2}+\frac{3}{2}(\frac{dR}{dt})^2=\frac{P(R)-P_\infty}{\rho_1}-\frac{2F}{\rho_1 R}-\frac{4\mu}{\rho_1 R}\frac{dR_b}{dt} \quad -------(3.0.3.3)$$

The growth of bubble radius is defined as:

$$\frac{dR}{dt}=\rho_{vap}\frac{\rho_1}{\rho}\,C(1-C)\frac{3}{R_b}\sqrt{\frac{2}{3}\frac{P_{vap}-P}{\rho_1}} \quad ------(3.0.3.4)$$

Where:

$P \rightarrow Local\ fluid\ pressure$

The bubble radius (R_b) for Schnerr-Sauer cavitation model is given by:

$$R_b=(\frac{C}{1-C}\frac{3}{4\pi}\frac{1}{n})^{\frac{1}{3}} \quad ------(3.0.3.5)$$

The volume of fraction used in Schnerr-Sauer cavitation model is given by:

$$C=\frac{n_o}{1+n_o\frac{4}{3}\pi R^3}\frac{d}{dt}(\frac{4}{3}\pi R^3) \quad ------(3.0.3.6)$$

where:

$n_o \rightarrow Number\ of\ seed\ per\ unit\ volume\ of\ liquid, V_v \rightarrow Volume\ of\ vapour$

Due the effect bubbles grow process; the flow is no longer divergence free but causes the curl of the velocity to transform into

$$\nabla.\vec{U}=\frac{\rho_v-\rho_1}{C\rho_v+(1+C)\rho_1}\frac{dC}{dt} \quad ------(3.0.3.7)$$

3.0.4 Turbulence Modeling: K-epsilon (k-ε) Model

Turbulence, a complex and unpredictable fluid flow phenomenon marked by significant momentum and energy exchange, poses challenges for direct simulation in numerous real-world scenarios, particularly at high Reynolds numbers. To overcome this, turbulence modeling techniques are utilized to approximate the effects of turbulence without fully resolving all flow scales. Among the various turbulence models, the k-ε model emerges as a

widely adopted and robust approach for engineering applications, owing to its simplicity, balanced accuracy, and computational efficiency.

In cavitation research, the k-ε turbulence model is widely employed to simulate the turbulent fluid dynamics within pumps and other hydraulic equipment so as to obtain correct and reliable results. Turbulent fluctuations in the fluid play a significant role in the formation and collapse of vapor cavities, which are fundamental to the cavitation phenomenon. Numerous prominent studies on cavitation using CFD techniques such as (Luo et al., 2022), (Orlandi et al., 2023a), (C. Li et al., 2023a) have utilized the k-ε model as the turbulence modeling approach in their investigations.

Turbulent flows involve a wide spectrum of scales, from large eddies, which contain most of the kinetic energy, to smaller eddies, where energy dissipates as heat due to viscosity. Directly solving the Navier-Stokes equations, which govern fluid flow, becomes computationally impractical for turbulent flows as it requires resolving all turbulent scales. To simplify the problem, Reynolds-Averaged Navier-Stokes (RANS) equations are employed, which decompose flow variables into mean and fluctuating components. This leads to the introduction of the Reynolds stress tensor, which represents the effects of turbulence. Turbulence models, such as the k-ε model, are developed to close the RANS equations by relating the Reynolds stresses to the mean flow properties.

The k−ε model is a two-equation turbulence model that solves two transport equations: one for the turbulent kinetic energy (k) and another for its dissipation rate (ε). This approach allows the model to account for the transport of turbulence properties and their interaction with the mean flow.

i. The **turbulent kinetic energy (k)** represents the intensity of turbulence, and its equation is given by:

$$\frac{\partial \kappa}{\partial t} + U_j \frac{\partial \kappa}{\partial x_j} = \frac{\partial}{\partial x_j}\left[\left(\nu + \frac{\nu_\tau}{\sigma_k}\right)\frac{\partial k}{\partial x_j}\right] + \tau_{ij}\frac{\partial U_i}{\partial x_j} - \varepsilon \quad \ldots\ldots\ldots\ldots\ldots (3.0.4.1)$$

$Where$:

$\tau_{ij}\frac{\partial U_i}{\partial x_j}$: $Production\ of\ turbulent\ kinetic\ energy$

ν_τ: $Turbulent\ viscosity\ = C_\mu \frac{k^2}{\varepsilon}$

σ_k: $Prandtl\ number\ for\ k$

ii. The **dissipation rate (ε)** represents the rate at which turbulent kinetic energy is converted into thermal energy due to viscous dissipation, and its equation is given by:

$$\frac{\partial \varepsilon}{\partial t} + U_j \frac{\partial \varepsilon}{\partial x_j} = \frac{\partial}{\partial x_j}\left[\left(\nu + \frac{\nu_\tau}{\sigma_\varepsilon}\right)\frac{\partial \varepsilon}{\partial x_j}\right] + C_{\varepsilon 1}\frac{\varepsilon}{k}\tau_{ij}\frac{\partial U_i}{\partial x_j} - C_{\varepsilon 2}\frac{\varepsilon^2}{k} \ldots\ldots\ldots\ldots\ldots (3.0.4.2)$$

$Where$:

σ_ε: $Prandtl\ number\ for\ \varepsilon$

$C_{\varepsilon 1}, C_{\varepsilon 2}\ are\ Closure\ coefficients$

The k – ε model employs the following standard constants, determined empirically:

$$C_\mu = 0.09, \sigma_k = 1.0, \sigma_\varepsilon = 1.3, C_{\varepsilon 1} = 1.44, C_{\varepsilon 2} = 1.92$$

While standard k−ε model (discussed above), is robust and widely used, limitations exist in accurately capturing certain complex flow phenomena, such as flows with high strain rates, strong curvature, or rotational effects. To address these challenges, advanced variant such as the RNG k−ε was utilized in our simulation.

I. RNG k−ε Model

The RNG k-ε model (Re-Normalization Group), a more recent version of the k-ε model developed by Yakhot and Orszag (1986) which enhances the standard k-ε model by incorporating additional terms derived from renormalization group theory, improving accuracy in rapidly strained and swirling flows. Similar to the standard model, the eddy viscosity, k and ε are still given by Equations (3.0.4.1) and (3.0.4.2). However, the model uses a modified coefficient, $C_{\varepsilon 2}$, defined by

$$C_{e2} \equiv \bar{C}_{e2} + \frac{C_\mu \lambda^3 \left(1 - \frac{\lambda}{\lambda_o}\right)}{1 + \beta\lambda^3}, \qquad where, \qquad \lambda = \frac{k}{\varepsilon}\sqrt{2S_{ji}S_{ij}}$$

The closure coefficients for the RNG k-ε model becomes:

$$C_\mu = 0.085, \sigma_k = 0.72, \sigma_\varepsilon = 0.72, C_{\varepsilon 1} = 1.42, \bar{C}_{e2} = 1.68, \beta = 0.012, \lambda_o = 4.38$$

This formulation allows the RNG k-ε model to adapt dynamically to flow characteristics, making it particularly useful for high-shear and rotating flows where cavitation is prevalent. The interaction of turbulence with cavitation is very complex, as turbulence both affects and is affected by cavitating flows. For example, the turbulent fluctuations may induce pressure variations that lead to the formation of vapor cavities, while cavitation itself may alter the turbulence structure. Hence, the need of using the RNG k-ε model in conjunction with a cavitation model (such as the Schnerr-Sauer bubble model discussed in 3.0.3) providing a robust approach for our analysis.

3.1 Computational Fluid Dynamics (CFD) Approach

3.1.1 Overview of the CFD Workflow

To ensure precision in our investigation, the workflow detailed in Fig. 3.1.1.1 was carefully developed to serve as a guiding framework. This flowchart, grounded in the standard CFD analysis methodology utilized by fluid dynamics researchers, effectively captures the sequential stages of the study. From the initial geometry creation and defeaturing to the meshing process, solver setup, and ultimately the convergence of the analysis, the flowchart concisely summarizes the entire process.

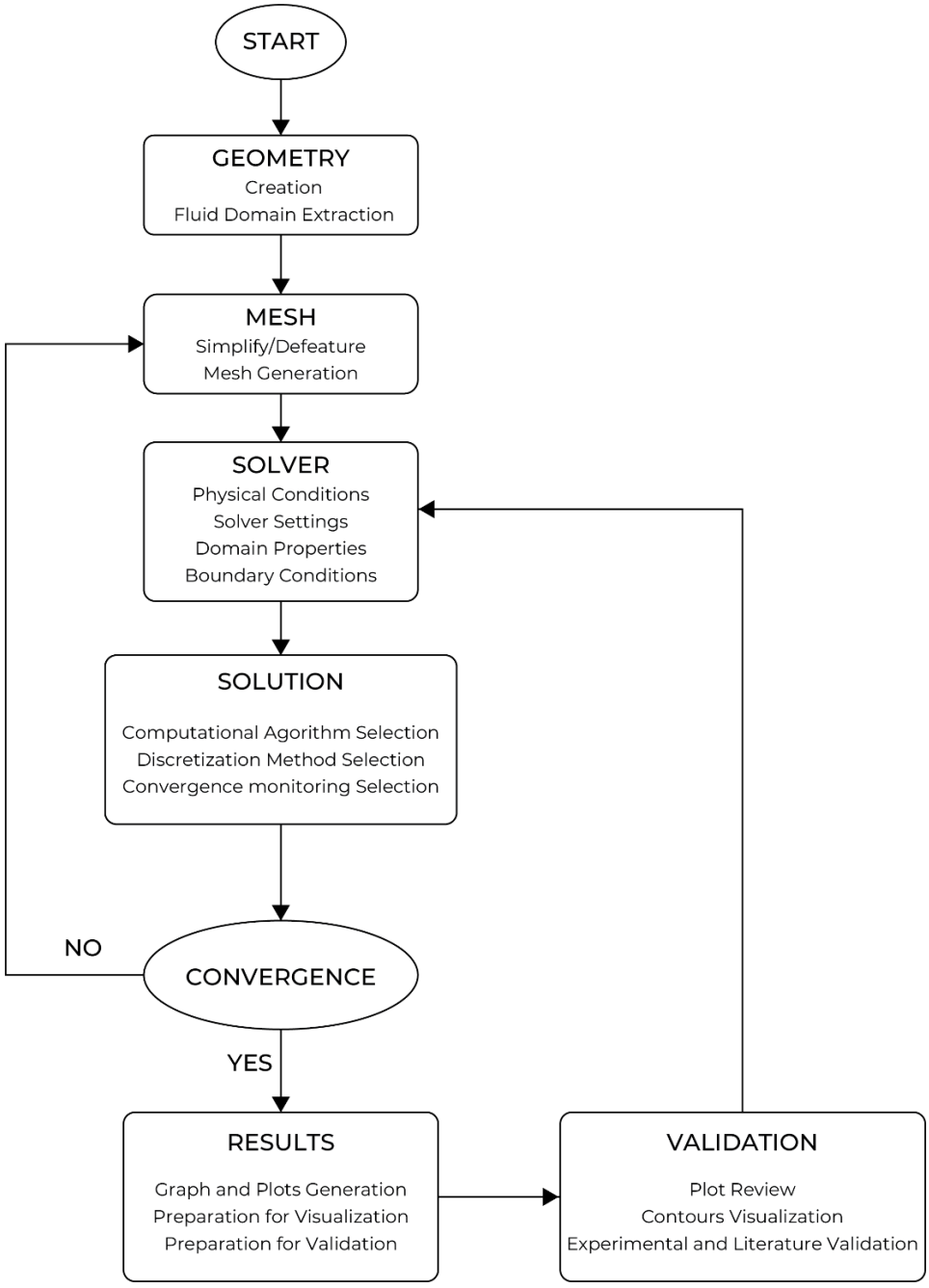

Figure 3.3: Flowchart illustrating this study workflow

Following this systematic approach, the workflow guarantees consistency and methodological rigor throughout the project. It highlights the critical steps necessary to accurately model and analyze complex fluid flow problems such as cavitation analysis. This structured guide not only enhances the clarity of the study but also aligns with best practices in CFD research, ensuring reliable and reproducible results.

3.1.2 Geometry Definition

I. Geometry Creation

The geometry creation process in SolidWorks was guided by accurate dimensional data obtained from the technical datasheets and specifications provided by Flowserve®, a renowned manufacturer of industrial pumps. The Flowserve-6HPX15A API Pump (*Fig. 3.4*) dimensions, along with design and performance specifications, were sourced from publicly available resources, including the official Flowserve website, which supplies comprehensive details on their pump models. Key dimensions such as impeller diameter, blade angles, volute casing dimensions, suction and discharge port sizes, and the overall pump assembly layout were meticulously extracted to ensure the modeled geometry closely represents the real-world pump.

Figure 3.4: Flowserve-6HPX15A API Pump from an Online Store

These dimensions were verified against the datasheet we were provided by a well-known Oil and gas operator in Nigeria, to ensure consistency and accuracy. Once the dimensional data was consolidated, it served as the foundation for building the geometry in SolidWorks.

Figure 3.5: Flowserve-HPX Series API Pump from the company catalogue

Using SolidWorks, the main components of the Worthington® R Slurry Pump were modeled, including the impeller, volute casing, suction and discharge ports, and shaft assembly. Sketching tools and 3D operations, such as extrusion and rotation, were used to construct the components.

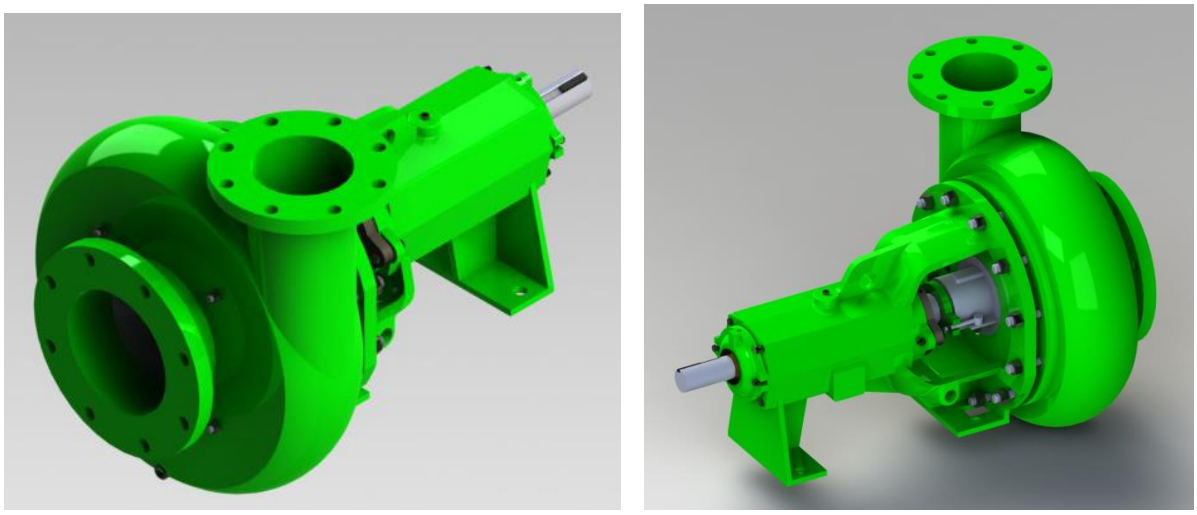

Figure 3.6: Modelled Geometry in SolidWorks

II. Defeaturing

Defeaturing involves simplifying a geometry by removing unnecessary details that do not significantly impact the simulation results. Defeaturing our pump model above involves excluding or removing features such as small fillets, chamfers, bolt holes, or fine surface textures to reduce computational cost and complexity, while prioritizing the impeller blades, volute casing, and suction/discharge ports as these regions are critical for capturing pressure changes and vapor bubble formation.

(a) (b)

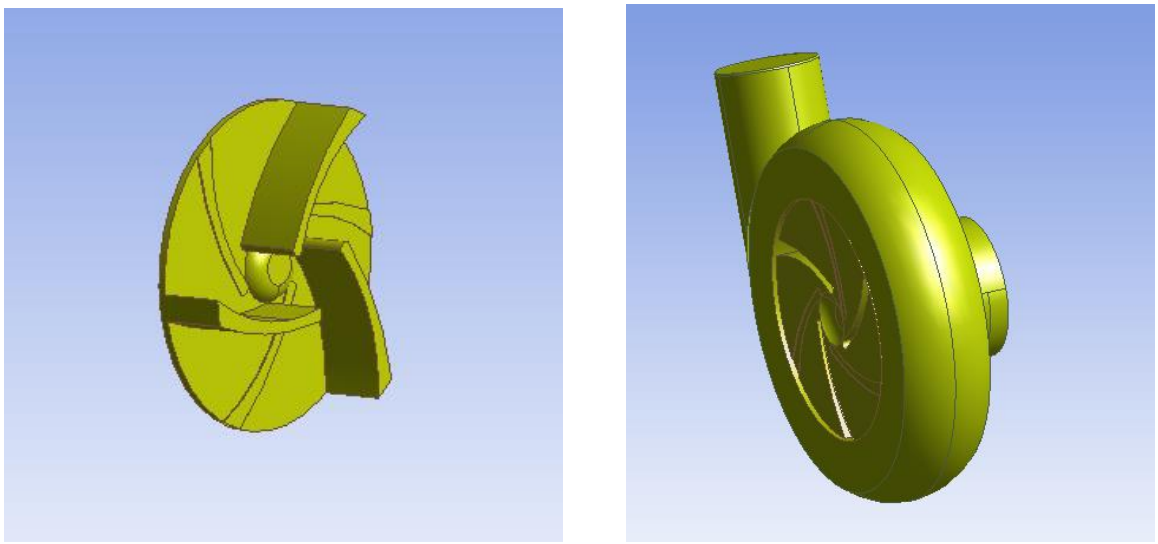

Figure 3.7: Defeaturing Process (a) Impeller defeaturing (b) Casing defeaturing

The aim is to create a model that retains the essential fluid flow paths and structural elements influencing cavitation while minimizing extraneous features that would unnecessarily increase the computational mesh density. This simplification improves solver efficiency and reduces memory requirements without compromising accuracy in areas of interest.

3.1.3 Domain Definition and Meshing

I. Fluid Domain Extraction

After defeaturing the geometric model, the next step involves isolating the region where the fluid interacts with the pump components, known as the fluid domain. This process involves subtracting the solid geometry of the pump's structural components such as the impeller, volute casing, and other internal features from a bounding volume representing the entire flow area. The resulting fluid domain serves as the foundation for the analysis.

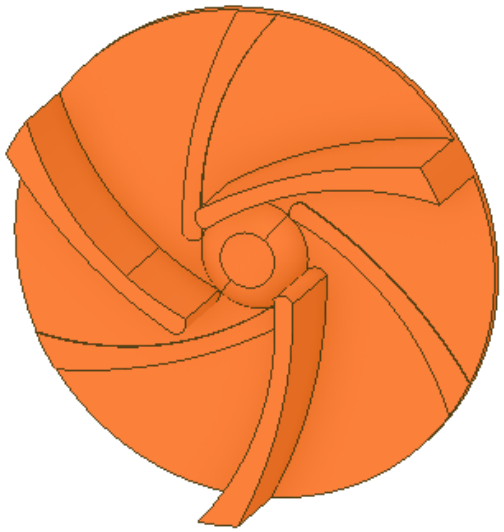

Figure 3.8: Fluid Domain Extraction - Front View of Impeller Fluid domain

The extracted fluid domain must accurately represent all critical flow regions, as proper fluid domain extraction ensures that the numerical simulation provides realistic predictions of flow behavior and cavitation effects while maintaining computational efficiency.

(a) (b)

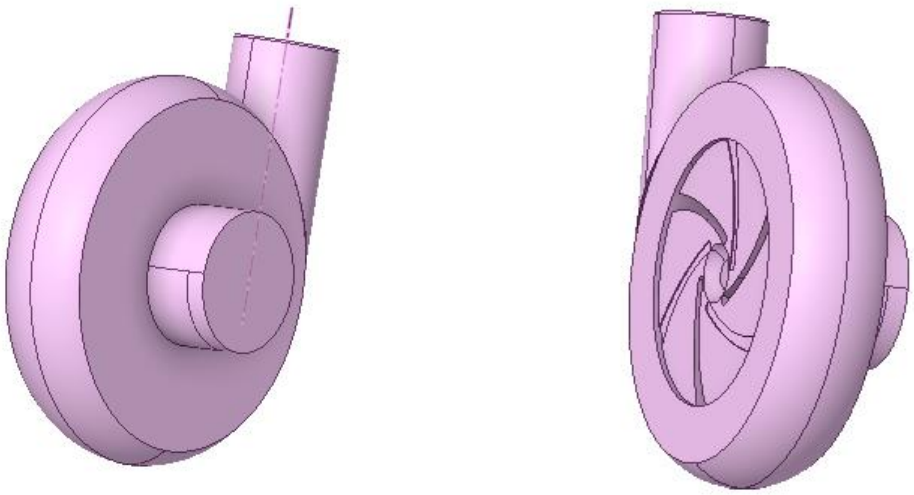

Figure 3.9: Fluid Domain Extraction (a) & (b) Front and Back view of Casing Fluid Domain

II. Meshing

Meshing involves discretizing the fluid domain into smaller elements, which form the basis for solving the governing equations of fluid flow. For the impeller Hexahedral 3D element with a sizing of 0.3cm was used, while for the casing fluid domain Tetrahedral 3D element with sizing of 1cm so as to account for the total number of element constraint in ANSYS Student License.

Mesh refinement (the process of increasing the density of elements) was then carried out in specific regions of interest, such as near the impeller blades, volute casing, and suction/discharge ports using ANSYS FLUENT adaptive meshing techniques.

Good mesh quality is crucial for simulation stability and accuracy, therefore quality metrics such as skewness, aspect ratio, and orthogonality were employed. Mesh independence tests was also conducted to confirm that further refinement does not significantly alter the results, ensuring an optimal balance between accuracy and computational effort.

(a) (b)

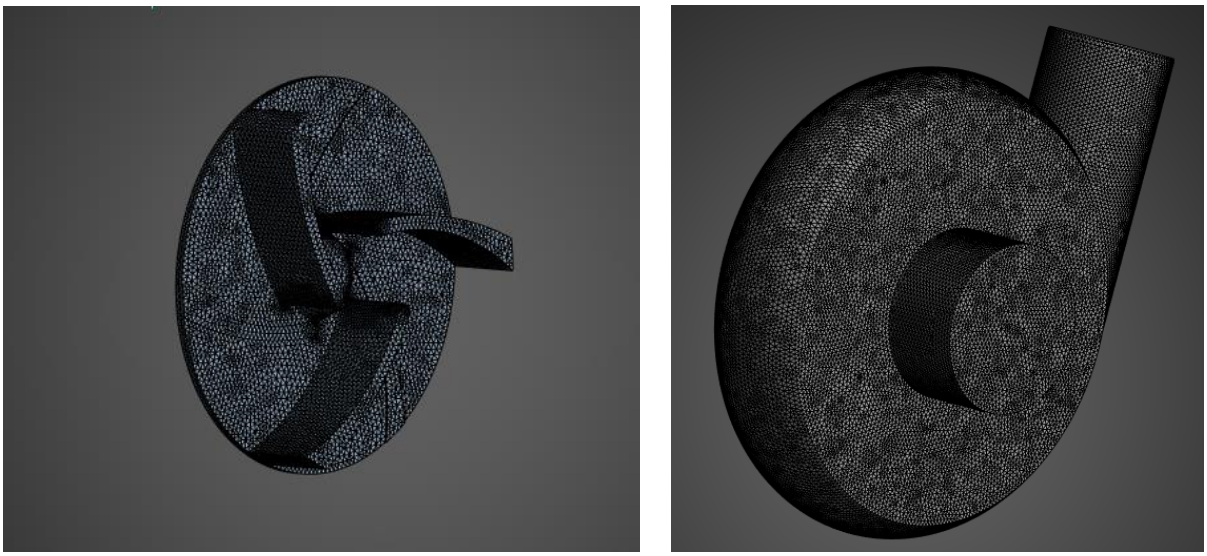

Figure 3.10: (a) Impeller Mesh (b) Casing Mesh

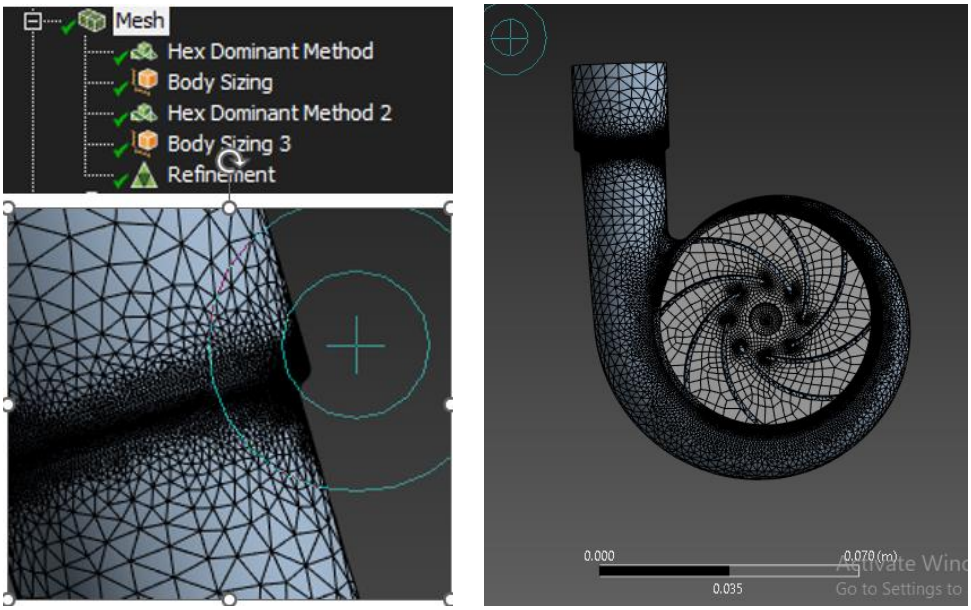

Figure 3.11: Mesh Refinement Setup

3.1.4 Data Collection and Extraction

The process of data collation and extraction involved organizing and analyzing pump performance data provided in a datasheet by a well-known oil and gas operator in Nigeria. This datasheet contained design and operational parameters, including flow rates, head, impeller dimensions, suction and discharge pressures, efficiency, and net positive suction head (NPSH) requirements for the centrifugal pump. The goal was to extract and structure this information systematically to support the cavitation analysis and model development.

Microsoft Excel was used as the primary tool for data collation due to its versatility in handling large datasets and its powerful analytical capabilities. Key parameters were organized into rows, with each column representing specific operating conditions. For instance, rows were created for flow rate (Q), head (H), and NPSHa, to ensure clarity and easy accessibility of the information.

Pump Parameters	**Raw Values from Datasheet**	**Converted Values**
Inlet Pressure (Gauge Value)	17.4 PSIG	221.39 kPa
Outlet Pressure (Gauge Value)	290.4 PSIG	2103 kPa
Operation Temperature	143F	60.7 C
Impeller Material	A 487 CA 6NM	
Casing Material	A 216 GR WCB	
Tip clearance thickness		
Angular Velocity of the Impeller	3565 rpm	261.6m/s
NPSHA/NPSHR	40/27.2 (ft)	12.192/8.2296 (m)
Discharge Flow rate	1680GPM	0.106 m3/s

Table 3-1: Pump parameters extracted from datasheet

Crude Oil Properties	**Raw Values from Datasheet**	**Converted Values**
Crude Oil Specific Gravity	0.8	800 Kg/m3
Vapour Dynamic Viscosity at the Operating Temperature	2.54 cP @ 60.7 C	0.0254 P
Crude Oil Dynamic Viscosity at the Operating Temperature	4.39cP @ 22.2 C	0.0439 P
Surface Tension		0.0594 N/m
Vapour Pressure	17.5 PSIA @ 60.7 C	120.66 kPa
Vapour Density		5.21kg/m3
Inlet velocity to the pump	10980Ft/hr	0.934 m/s.

Table 3-2: Crude oil Properties extracted from datasheet

This organized and extracted data was instrumental in defining boundary conditions and input parameters for subsequent CFD simulations.

3.1.5 Solver Setup

I. Boundary Condition Setup

The fluid inlet velocity is set as ".934m/s", the outlet pressure is as "2103kPa" and the impeller angular velocity as "3565 rev/min" in the x-axis. To account for the motion of the impeller at every time step, a mesh motion algorithm was used. The operating temperature for this simulation is "60.7 degree Celsius".

For turbulence specification, "the intensity and viscosity ratio" was used with a turbulent intensity [%] of "5" and turbulent viscosity ratio of "10". For the phase (liquid crude oil and vapor crude oil) properties present in the simulation, the density and viscosity were set. For the liquid phase, a density of 800 kg/m^3" and a viscosity of "4.39 cP" and for the vapour phase, a density of "5.21 kg/m^3" and a viscosity of "2.54 cP".

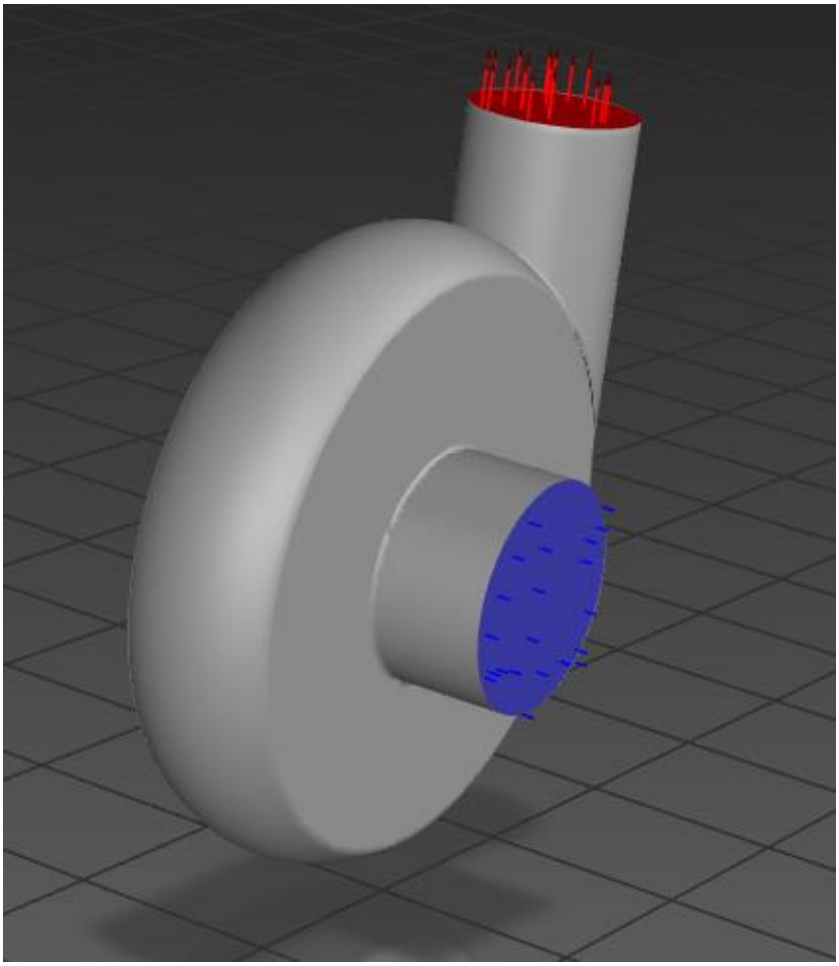

Figure 3.12: Fluid domain showing the inlet and outlet of fluid flow

II. General Simulation Setup

For the simulation conducted, the pressure-based solver was used alongside with the Absolute value for the velocity formulation. Since cavitation involves transport of bubbles, a transient time model was used. Also applying gravitation to account for the effect of gravity.

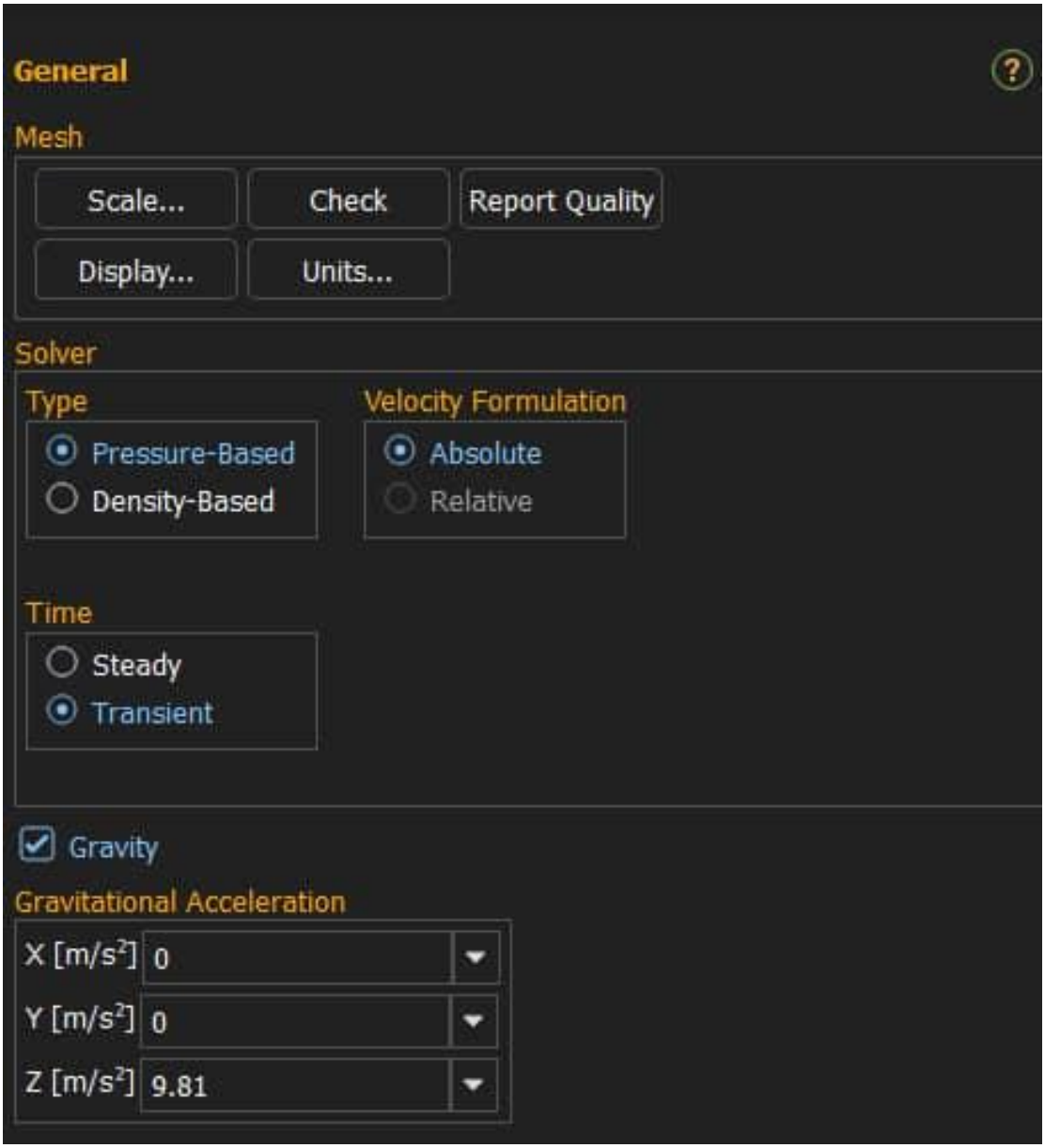

Figure 3.13: General setup

For the model setup, volume of fluid model (VOF) was used. Also to get a sharp interface between phase in the simulation the "sharp" interface model was used. The courant number (C.N) used for simulation is ".25" and volume of fraction cutoff is "10^{-6}". For the interaction between the phases, a surface tension coefficient of "0.0594 N/m" was used while the cavitation a mass transfer mechanism was set between phases.

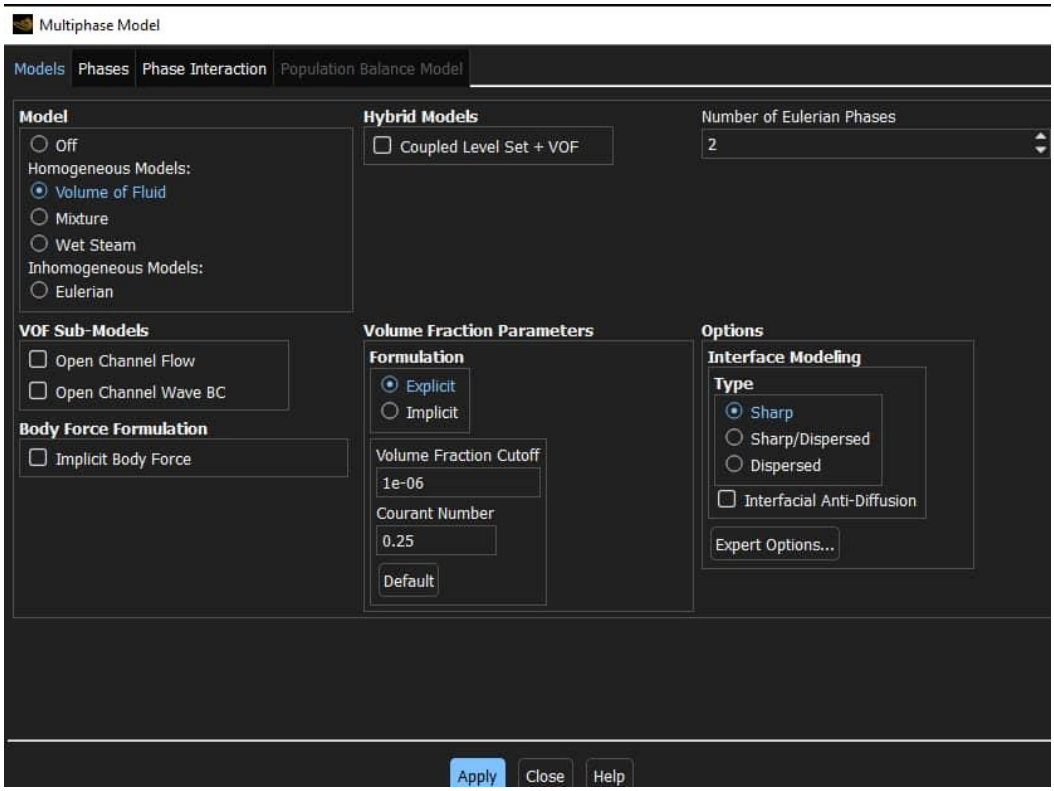

Figure 3.14: Volume of fluid setup (i)

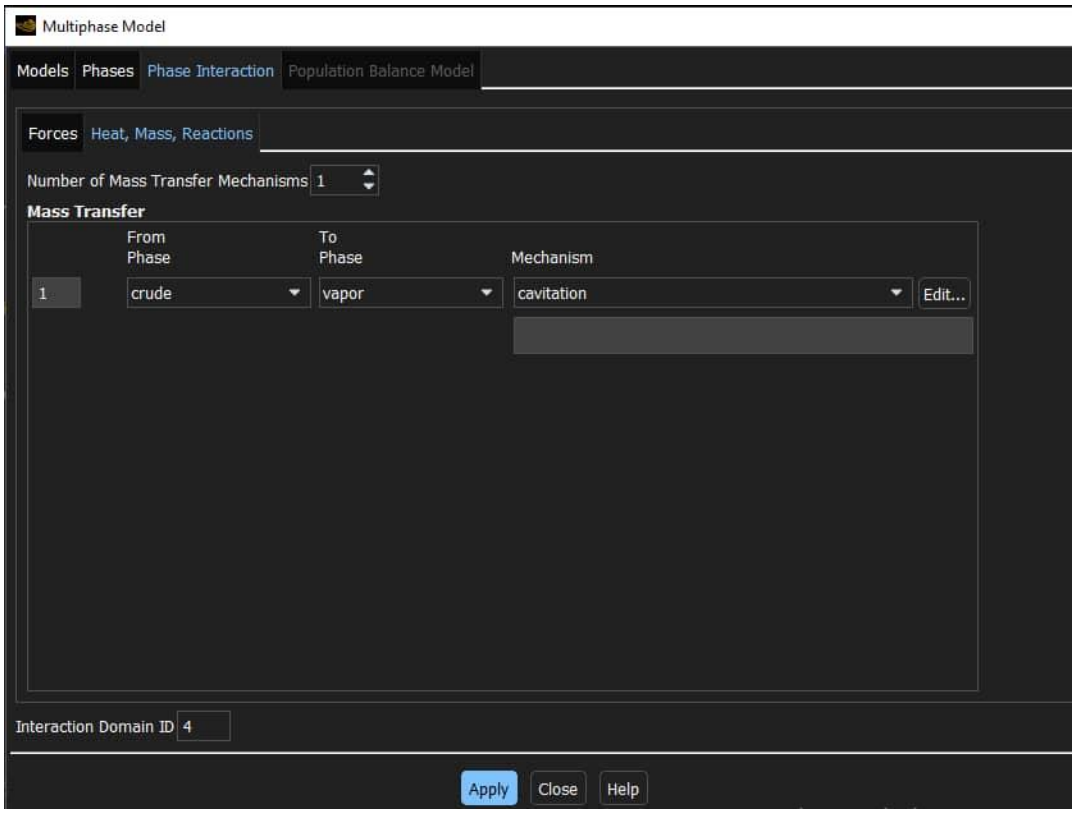

Figure 3.15: Volume of fluid setup (ii)

For the viscous model setup, k-epsilon realizable model was used, with model constant value as given below:

$$C_2 - Epsilon = 1.9, TKE\ prandtl\ number\ = 1, TDR\ prandtl\ number\ = 1.2$$

To account for the wall characteristic, “standard wall function” near- wall treatment was chosen in the viscous model setup.

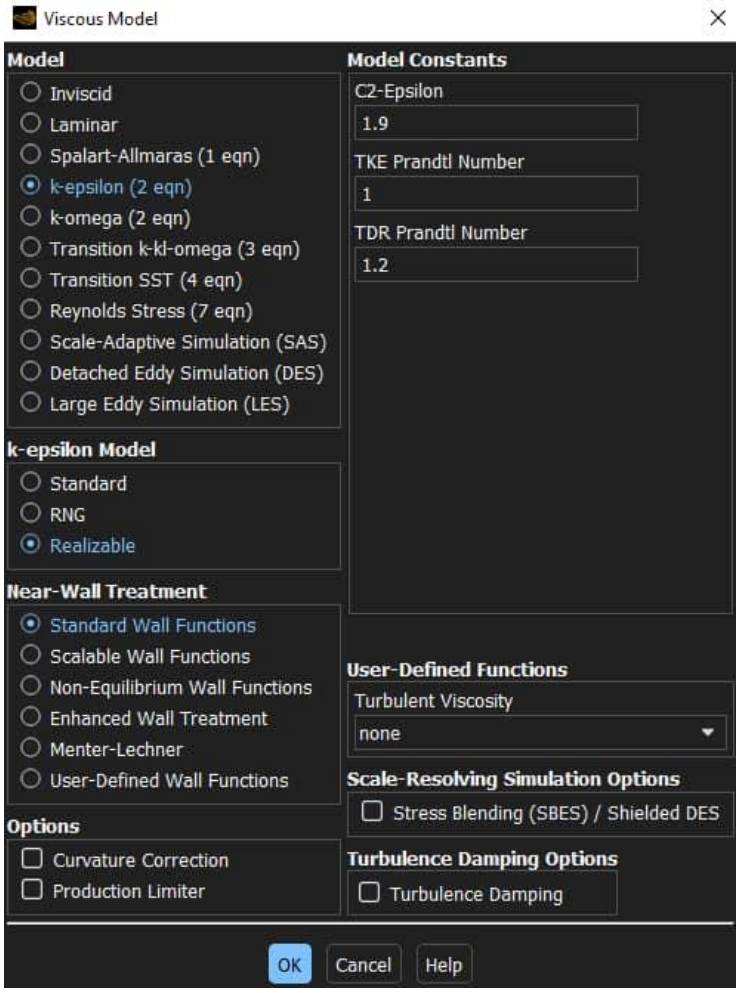

Figure 3.16: Viscous model setup

For the solution method set up, the image below shows the value assigned to the pressure-velocity coupling algorithm which determine the relationship of the pressure and velocity of the fluid domain for each iteration, and the spatial discretization algorithm which determine the method of tracking the interface.

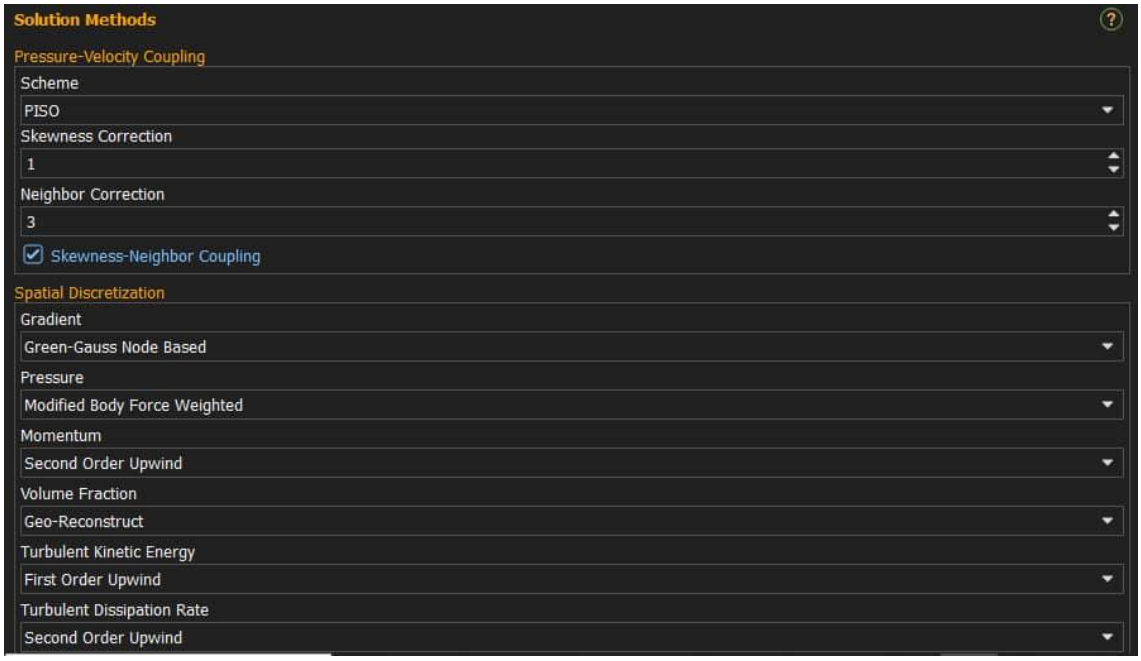

Figure 3.17: Solution method setup

In order to control the solution outcome of the simulation, the under-relaxation factors were set which is shown in the image below.

Figure 3.18: Solution control setup

To monitor the convergence of the computational fluid dynamic equation, the residual for each iteration was set, the image below shows the setup done.

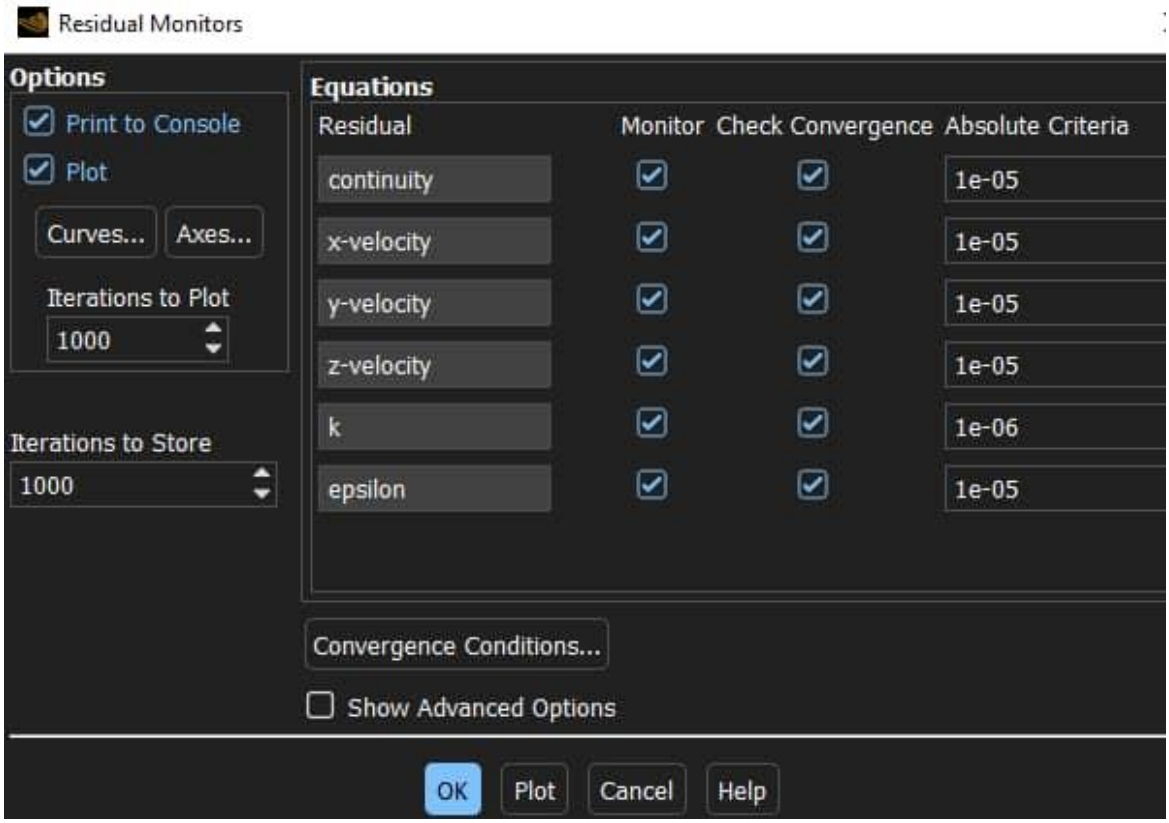

Figure 3.19: Residual monitor setup

CHAPTER 4

RESULTS AND DISCUSSION

4.0 Results

This chapter presents the results obtained from the simulations based on the data and methodologies outlined in Chapter 3. Multiple simulation iterations were conducted, and three key cases will be analyzed in this chapter. The results will be discussed under two critical categories namely; Pressure Distribution Analysis and Vapor Volume Fraction Analysis. Each category provides insights into the effects of cavitation on the pump's performance, highlighting variations in pressure and vapor formation under different conditions.

4.0.1 Pressure Distribution Analysis

In this section, the results of each simulation iteration are analyzed in terms of pressure distribution. The pressure distribution analysis provides insight into how pressure varies throughout different sections of the centrifugal pump, from the inlet to the outlet. In an ideal scenario, the pressure gradually decreases from the pump inlet to the outlet. However, in regions where cavitation occurs, the pressure drops significantly, often falling below the vapor pressure of crude oil. This leads to the formation of vapor cavities, which impact the pump's performance and efficiency.

The following subsections presents pressure contour plots and graphs that illustrate these variations for the selected simulation cases.

I. Iteration 1

In this iteration, the simulation was performed under the assumption that the pump casing walls are completely smooth, meaning the roughness value was set to zero. To evaluate the impact of different fluid interactions on cavitation and pressure distribution, two sub-iterations were carried out:

1. **Sub-Iteration 1:** The simulation considered only the liquid phase (crude oil) and vapor phase, allowing an initial assessment of cavitation formation in the absence of air entrainment.

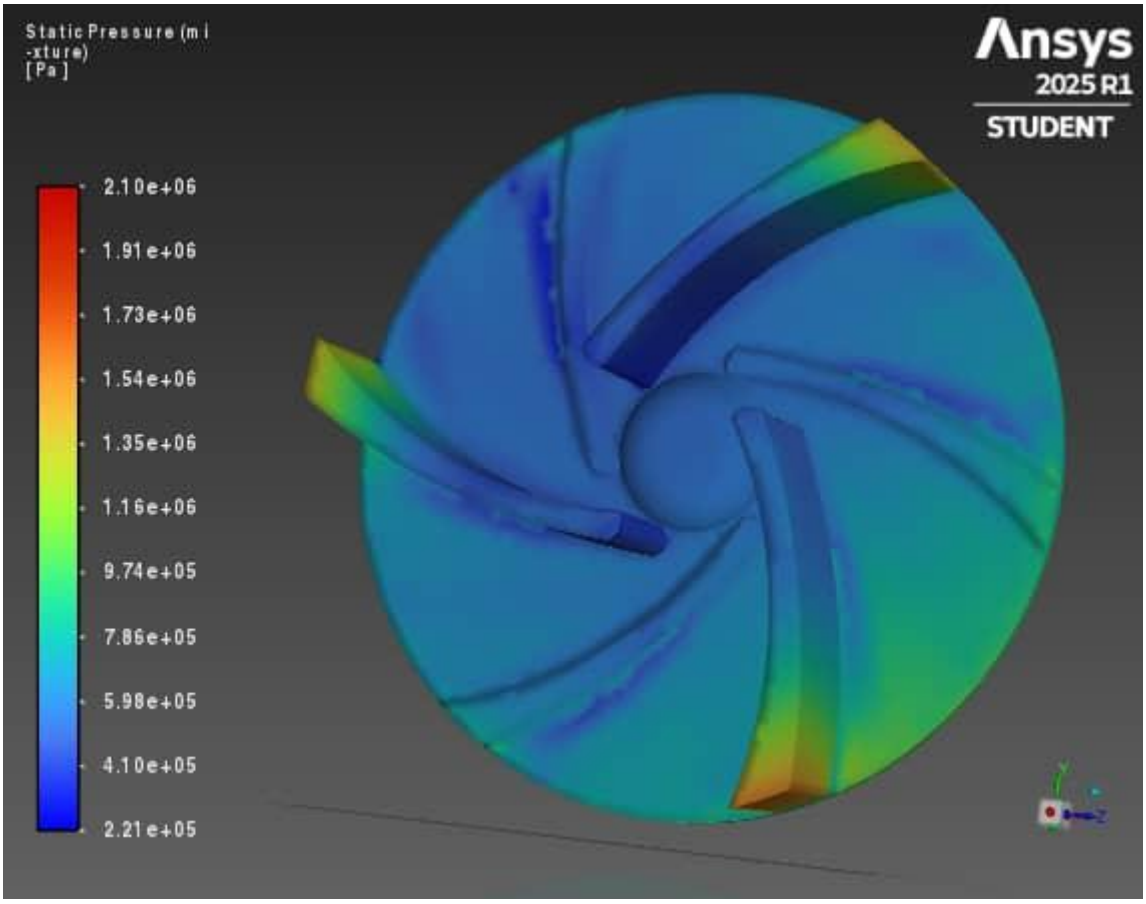

Figure 4.1: Impeller Pressure Contour for Sub-iteration 1

Figure 4.1 shows the pressure distribution in the pump when only crude oil and vapor are considered.

From the pressure distribution:

i. The highest pressure is observed at the pump inlet.

ii. There is no pressure drop in the impeller or casing indicating the absence of cavitation

2. **Sub-Iteration 2:** Air was incorporated into the medium to better replicate real-life operating conditions, where dissolved gases and entrained air may influence cavitation dynamics.

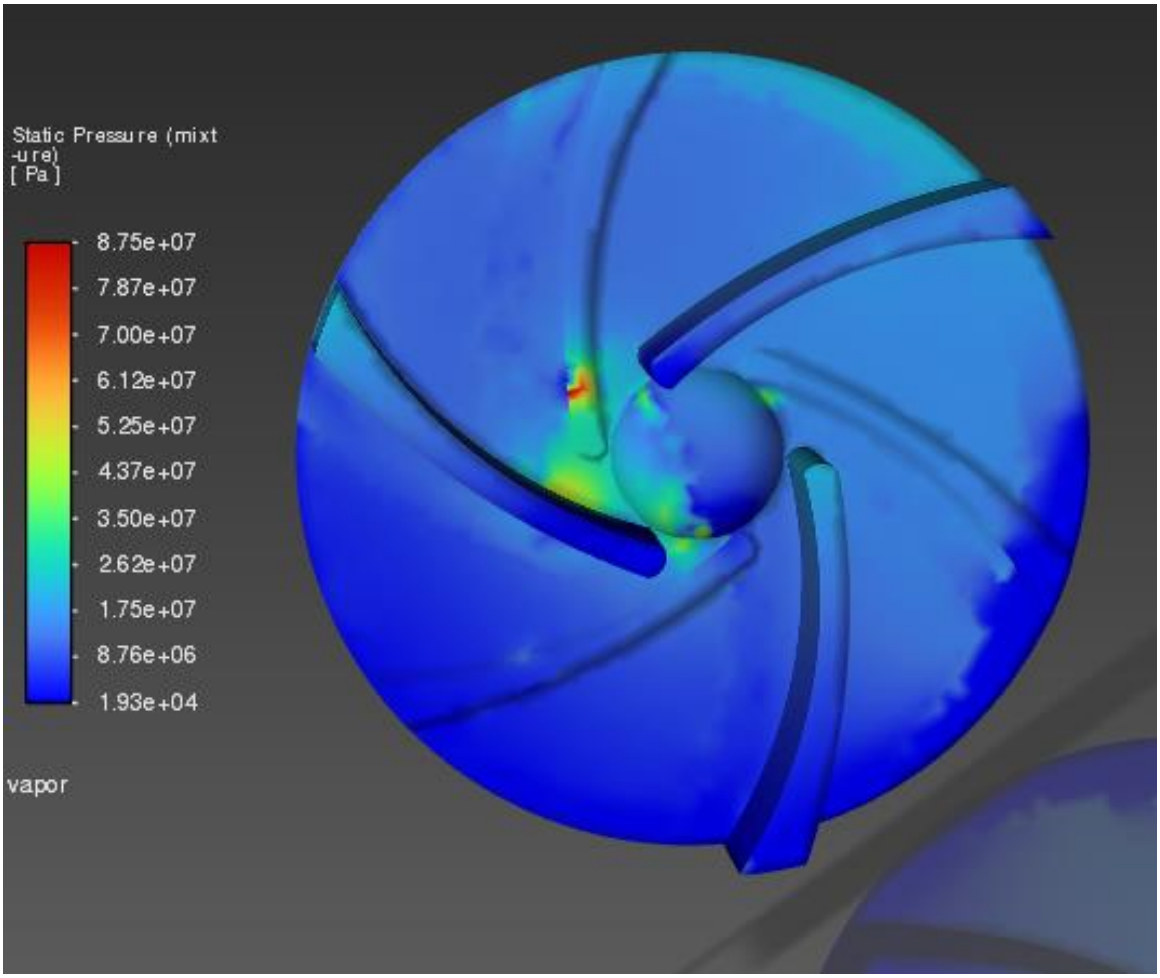

Figure 4.2: Impeller Pressure Contour for Sub-iteration 2

Figure 4.2 presents the pressure distribution when air is incorporated into the medium and the following key observations was made:

i. The pressure distribution pattern remains similar, but with noticeable differences in cavitation regions.

ii. The presence of air affects the extent and intensity of cavitation, slightly modifying the pressure drop across the impeller.

iii. Air entrainment tends to stabilize cavitation bubbles, delaying their collapse and potentially influencing pump performance.

Numerical Comparison of Pressure Values

Location	Sub-Iteration 1 Pressure Values (kPa)	Sub-Iteration 2 Pressure Values (kPa)
Inlet	221.39 kPa	221.39 kPa
Impeller Leading Edge	1400 kPa	2300 kPa
Cavitating Region	250 kPa (No cavitation)	105 kPa
Outlet	2103 kPa	2103 kPa

Table 4-1: Pressure Distribution Comparison for Sub-Iteration 1&2

From the table:

i. The inlet pressure remains consistent for both cases.

ii. The pressure at the impeller leading edge drops significantly, leading to cavitation.

iii. The presence of air slightly alters the pressure in cavitation-prone regions, affecting bubble dynamics and potentially reducing the severity of cavitation damage.

II. Iteration 2

In this iteration, the simulation was performed with a casing roughness value of 0.00015 m to assess the impact of surface roughness on cavitation behavior. Additionally, the Volume of Fluid (VOF) backflow conditions were set as follows: (a) Air VOF: 0.2 and (b) Crude Oil Vapor VOF: 0.8. These conditions were chosen to simulate realistic operational scenarios where air and vapor interact with the crude oil flow, influencing cavitation dynamics.

The pressure distribution for this iteration is presented in Figure 4.3 & 4.4 and the following observations was made:

i. The roughness of 0.00015 m increases turbulence near the pump casing, slightly altering the pressure distribution.

ii. A more pronounced pressure drop occurs near the leading edge of the impeller blades, compared to the smooth-wall case.

iii. The presence of backflow, with 0.8 VOF crude oil vapor, intensifies cavitation in localized regions

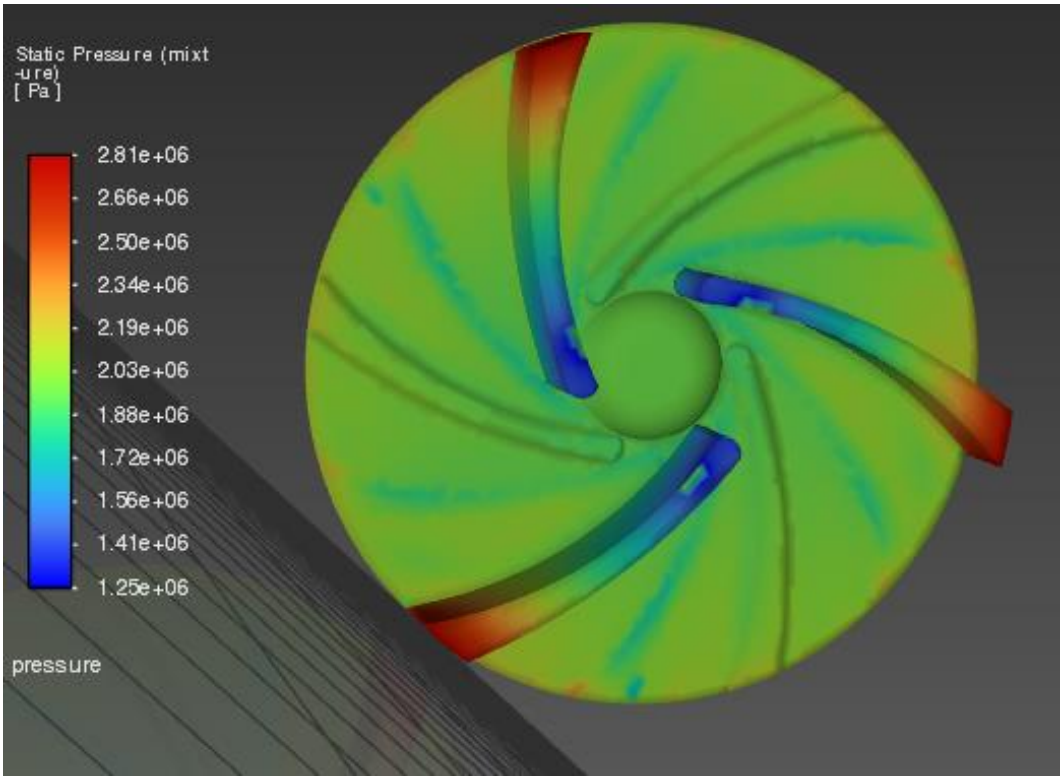

Figure 4.3: Impeller Pressure Contour for Iteration 2

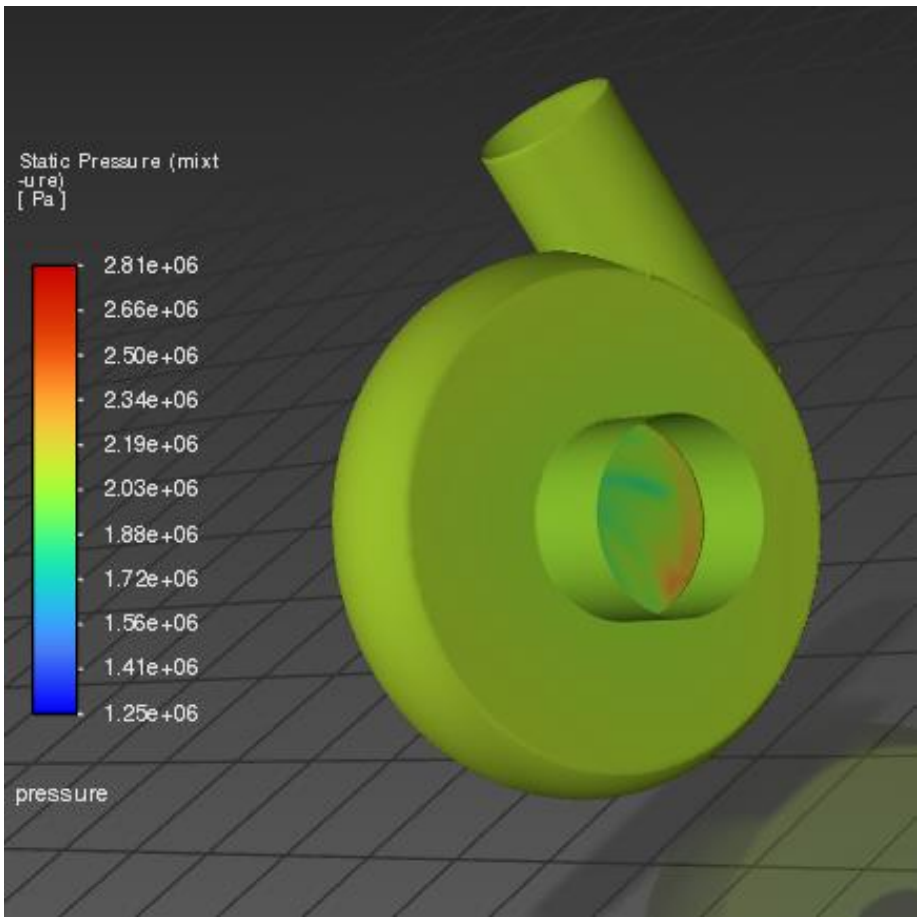

Figure 4.4: Casing Pressure Contour for Iteration 2

Numerical Comparison of Pressure Values

Location	Sub-Iteration 2 Pressure Values (kPa)	Iteration 2 Pressure Values (kPa)
Inlet	221.39 kPa	221.39 kPa
Impeller Leading Edge	2300 kPa	2810 kPa
Cavitating Region	105 kPa	115 kPa
Outlet	2103 kPa	2103 kPa

Table 4-2: Pressure Distribution Comparison for Sub-iteration 2 and Iteration 2

From the table, key observations include:

i. The impeller leading edge experiences a steeper pressure drop due to increased surface roughness and backflow effects.
ii. The cavitation region expands compared to Iteration One, indicating that roughness and backflow contribute to higher cavitation intensity.
iii. The outlet pressure remains relatively stable, though minor variations exist due to flow instability caused by cavitation.

III. Iteration 3

In this iteration, the pump casing roughness was set to 0.0015 m, representing a more realistic surface condition. Additionally, the Volume of Fluid (VOF) backflow conditions were adjusted as follows: (a) Air VOF: 1.0 (Full backflow of air) and (b) Crude Oil Vapor VOF: 0.0. This setup simulates a case where the pump experiences significant air entrainment, a condition that can occur due to improper sealing, suction issues, or operational inefficiencies.

The pressure distribution results for this iteration are shown in Figure 4.5 & 4.6 and the following key observations was made from the result:

i. The increased casing roughness of 0.0015 m causes more localized pressure fluctuations, leading to a greater pressure drop across the impeller.
ii. The introduction of full air backflow (VOF = 1.0) leads to significant changes in pressure distribution, particularly near the suction side.
iii. The low-pressure region expands, creating favorable conditions for cavitation onset in multiple zones of the pump.

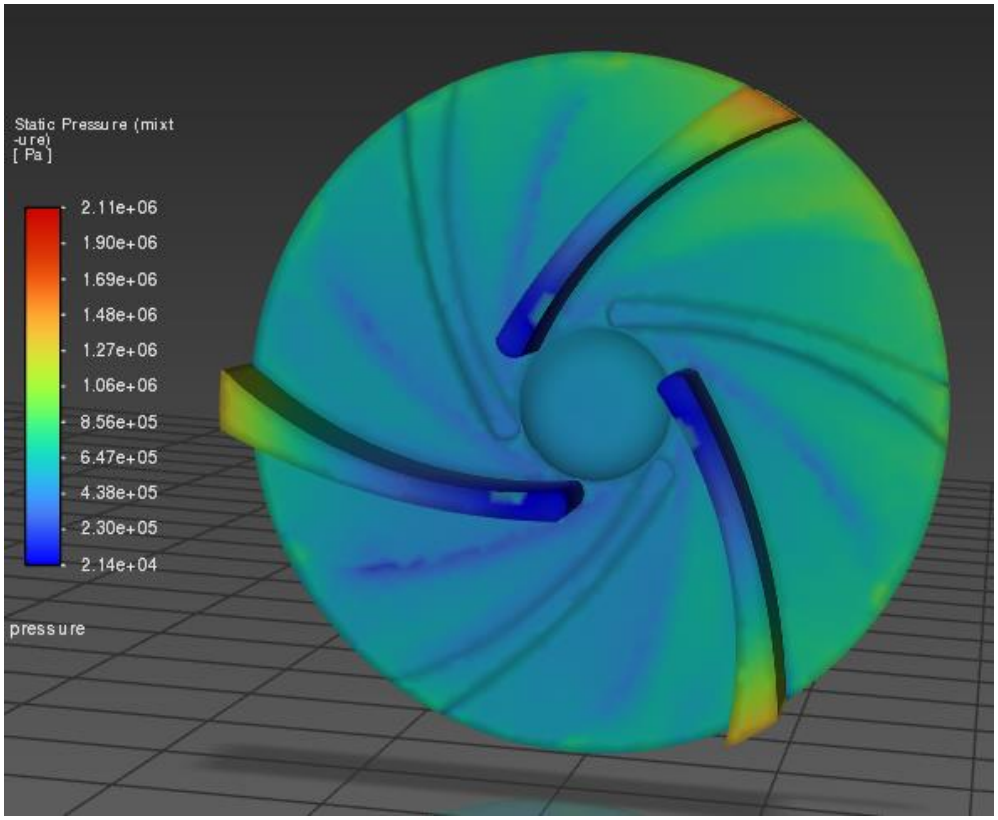

Figure 4.5: Impeller Pressure Contour for Iteration 3

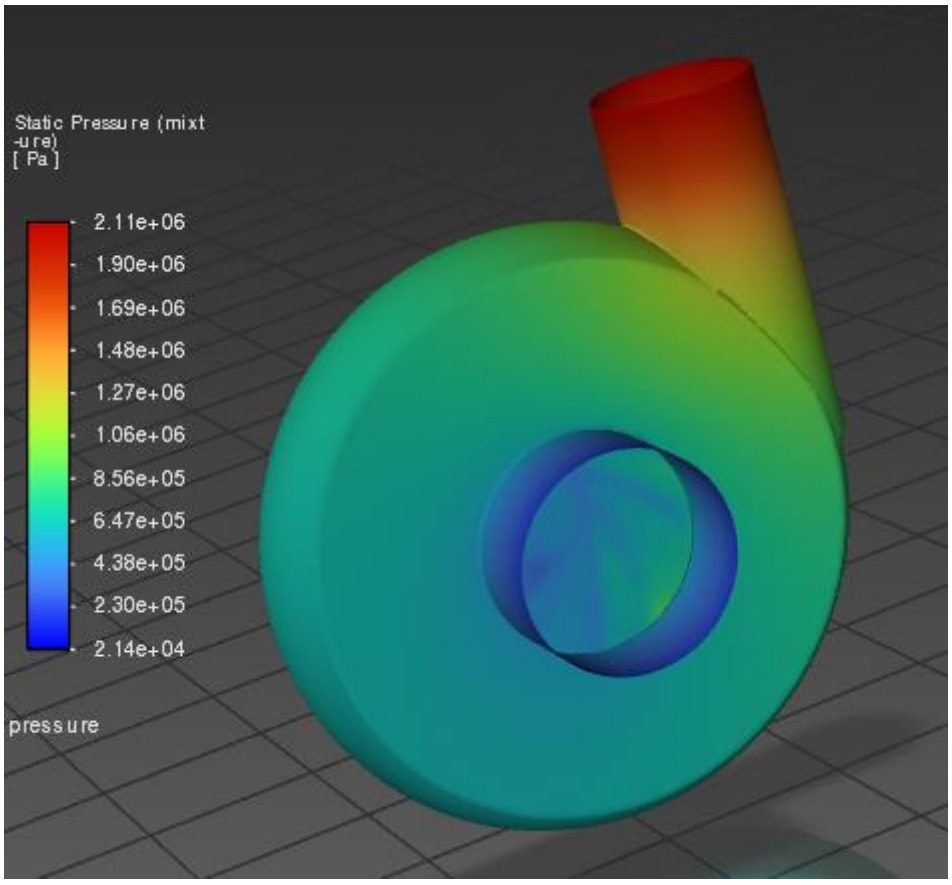

Figure 4.6: Casing Pressure Contour for Iteration 3

Numerical Comparison of Pressure Values

Location	Sub-Iteration 2 Pressure Values (kPa)	Iteration 2 Pressure Values (kPa)	Iteration 2 Pressure Values (kPa)
Inlet	221.39 kPa	221.39 kPa	221.39 kPa
Impeller Leading Edge	2300 kPa	2810 kPa	2110 kPa
Cavitating Region	105 kPa	115 kPa	21.4 kPa
Outlet	2103 kPa	2103 kPa	2103 kPa

Table 4-3: Pressure Distribution Comparison for Sub-Iteration 2, Iteration 2 & 3

Key insights:

i. The impeller leading edge pressure drops significantly due to increased surface roughness and entrained air, which disrupts the normal pressure recovery process.
ii. The cavitation region is larger compared to Iteration One, as air entrainment lowers local pressure, making cavitation more pronounced.
iii. The outlet pressure is reduced, indicating potential efficiency losses due to increased turbulence and flow disturbances.

4.0.2 Vapour Volume Fraction Analysis

The volume fraction of the incepting crude-oil vapour phase influenced by change in pressure distribution overtime resulting from change in backflow and roughness value was also investigated during the simulation.

In order to investigate the impact of backflow and geometry roughness on the formation and implosion of vapour bubbles, roughness height and the backflow volume of fraction (VOF) was altered during the analysis. The values used for the roughness parameter were at the range of the standard geometry roughness values for an actual industrial centrifugal pump used in the oil and gas sector.

The result for each iteration is given below:

I. Iteration 1

For this iteration, the geometry was assumed to be smooth (roughness height is approximately 0), having no vortex formation due to backflow (VOF=0). To evaluate the impact of different

fluid interactions on cavitation and vapour volume fraction, two sub-iterations were carried out:

1. **Sub-Iteration 1:** As stated previously in the pressure distribution analysis, this simulation considered only the liquid phase (crude oil) and vapor phase, allowing an initial assessment of cavitation formation in the absence of air entrainment.

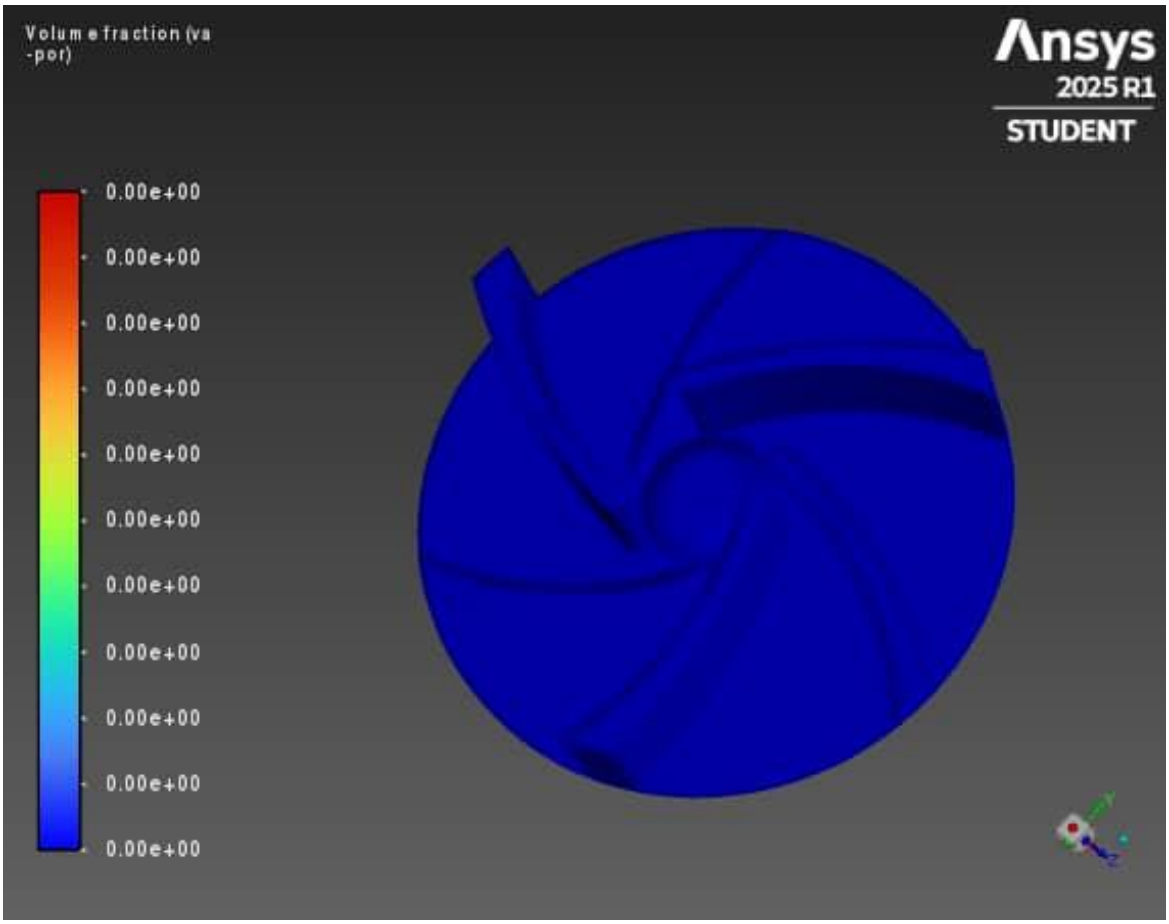

Figure 4.7: Impeller Vapour Volume Fraction Contour for Sub-iteration 1

From this analysis, the following was observed

i. The tendency of crude-oil vapour information in the geometry is low and due to a low probability of pressure drop along the geometry path.

ii. Reducing vorticity occurrence along the geometry path also reduces the formation of crude-oil vapour near the impeller.

2. **Sub-Iteration 2:** For this iteration, the roughness height used was .000015m and a backflow of zero (VOF=0) was used. This setup simulates a situation where although

the geometry has a minor roughness height but the formation of vortex does not occur along the path of the geometry.

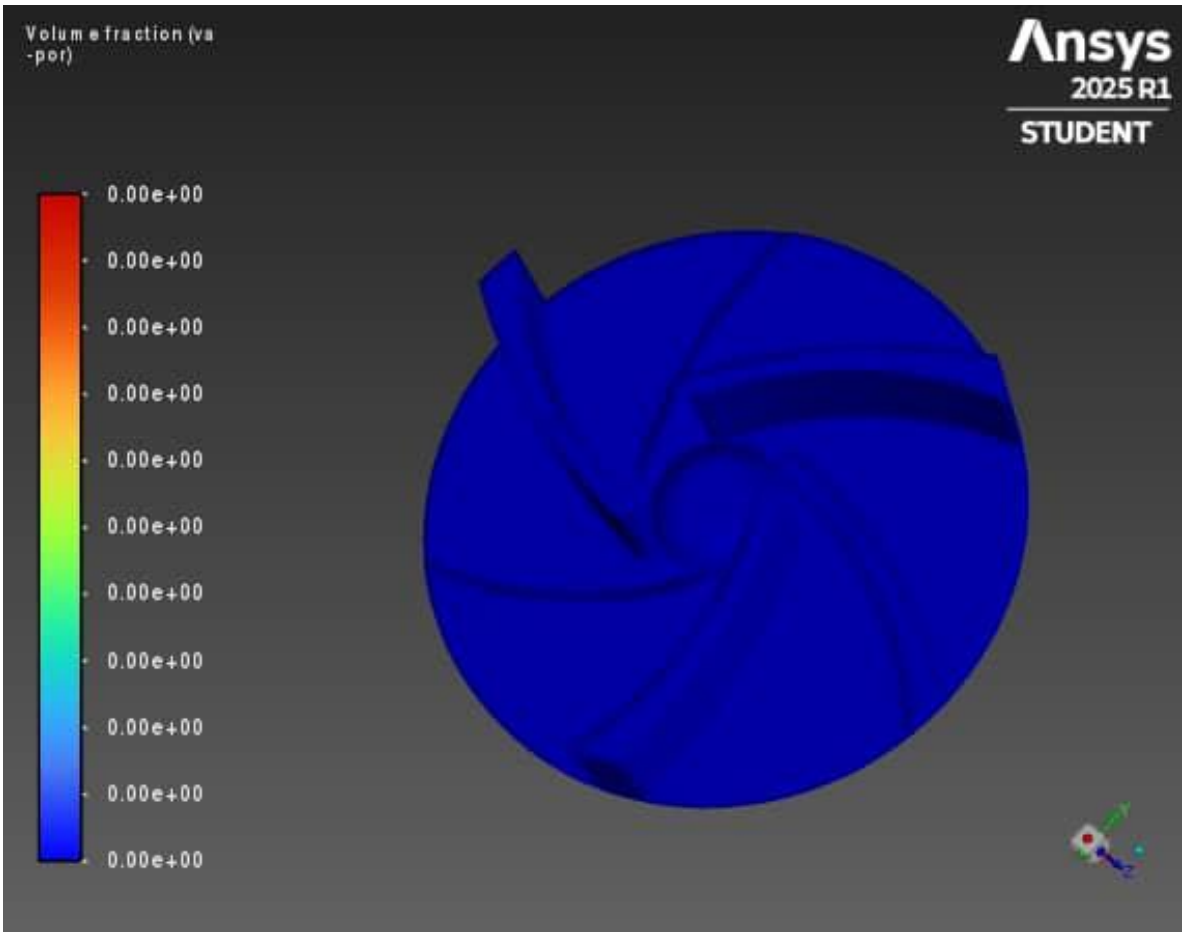

Figure 4.8: Impeller Vapour Volume Fraction Contour for Sub-iteration 2

This investigation using the setup above shows:

i. The roughness of the geometry causes a rise in the pressure drop along the geometry when compared to cases where the geometry is assumed smooth.
ii. Although this roughness increases the pressure drop, there is no formation or implosion of vapour bubbles along the geometry since the pressure do not drop below the vapour pressure of the crude-oil as shown in Figure 4.8.

II. Iteration 2

In order to get more insight of the effect of backflow on cavitation inception, in this iteration a roughness height of .00015m and a backflow of 0.2 (VOF=0.2) was used.

From fig 4.9 below, it can be observed that:

i. Vapour formation occurs when there is backflow of a phase (air in this case) along the geometry path

ii. This vapour occurs at the leading edge of the impeller blade.

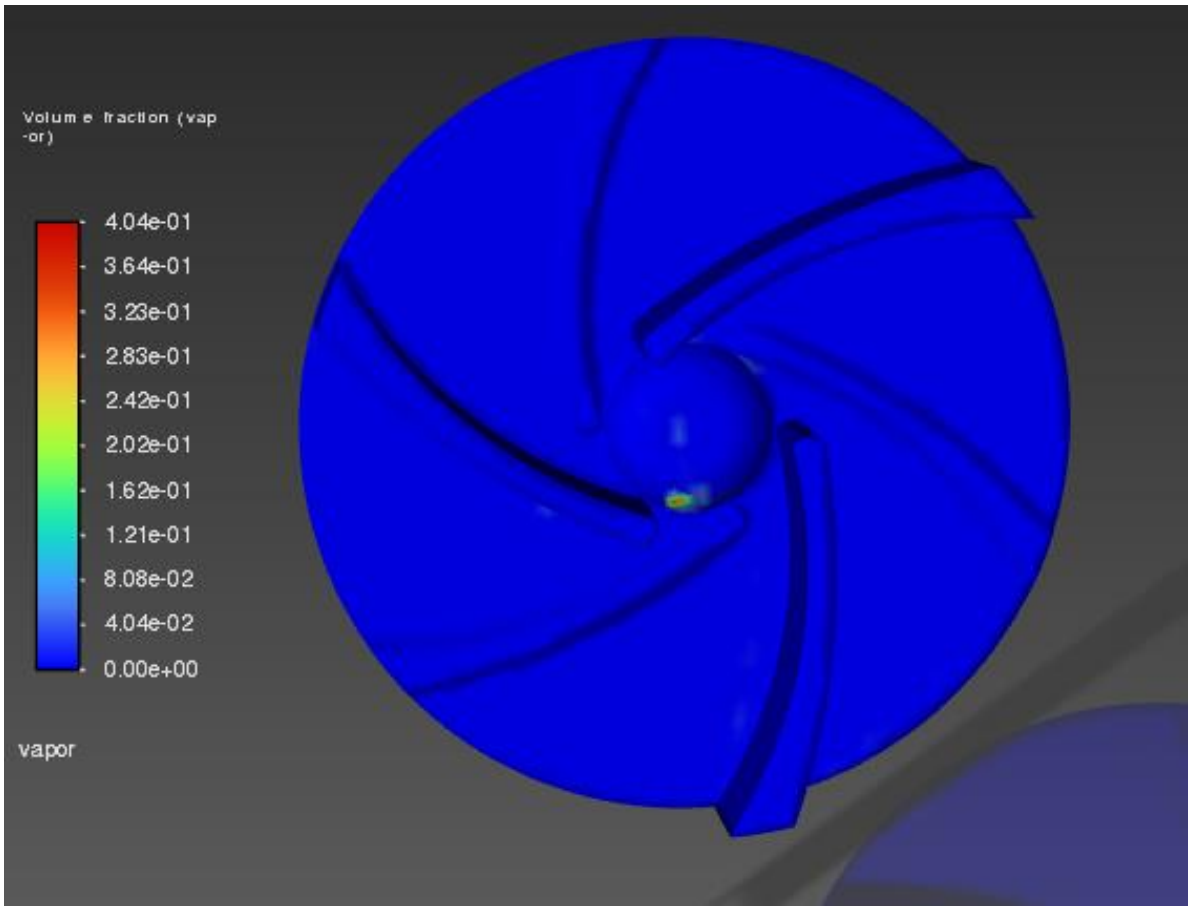

Figure 4.9: Impeller Vapour Volume Fraction Contour for Iteration 2

III. Iteration 3

In Order to investigate cavitation inception for a high critical case of the geometry path, a roughness height of .0015 and a backflow of 1 (VOF =1) was setup. This setup also includes the turbulence behavior of the phases in the geometry.

The result obtained due to this setup is shown in Figure 4.1.0. shows that

i. A high vortex formation along the centrifugal pump geometry results to a high formation of vapors.

ii. This vapour due to vortex implodes when a high energy is absorbed along the impeller geometry

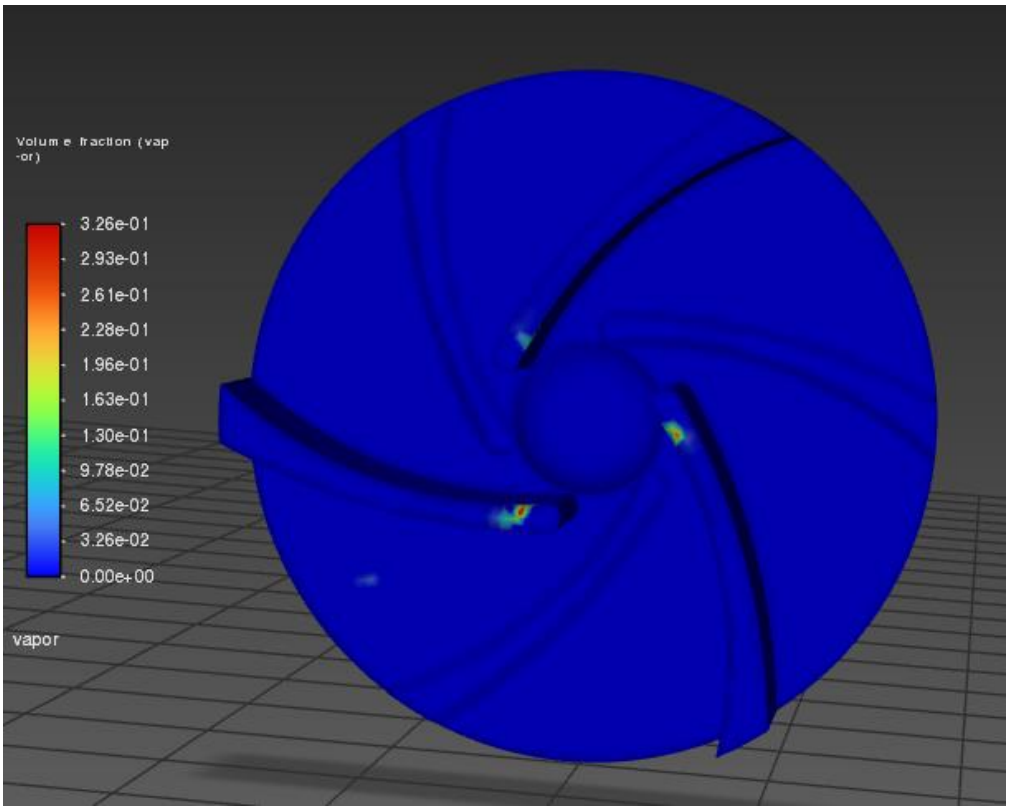

Figure 4.10: Impeller Vapour Volume Fraction Contour for Iteration 3

4.1 Discussion/Analysis of Results

This section provides a detailed analysis of the results obtained from the CFD simulations. The discussion focuses on the impact of cavitation on pump performance, the verification of the numerical approach through convergence and mesh independence tests, literature validation, and experimental validation.

4.1.1 Cavitation Effects on Pump Performance

Cavitation significantly influences the efficiency and lifespan of centrifugal pumps, especially in crude oil transportation. The simulation results show that cavitation occurs when the local pressure falls below the vapor pressure of crude oil, leading to the formation of vapor bubbles. These bubbles collapse violently, generating localized high-pressure zones that can erode pump components and reduce performance.

Key findings from the analysis include:

i. Surface Roughness Impact: As observed in Iteration Two and Three, increasing the pump casing roughness from 0.00015 m to 0.0015 m resulted in a more pronounced

pressure drop and an expansion of the cavitation zone. This indicates that pump surface conditions must be carefully controlled to minimize cavitation.

ii. Backflow Effects: The introduction of air backflow (VOF = 1.0) led to greater fluctuations in pressure distribution, promoting cavitation and reducing pump efficiency. This highlights the need for proper sealing and operational strategies to minimize air entrainment.

iii. Outlet Pressure Reduction: Compared to the smooth casing scenario, the outlet pressure decreased significantly in the rough casing cases, indicating potential energy losses and reduced pump head due to cavitation-related flow disruptions.

4.1.2 Verification: Convergence Test and Mesh Independent Study

To ensure the reliability of the CFD results, a convergence test and a mesh independence study were performed.

1. Convergence Test: The residuals of velocity, pressure, and volume fraction equations were monitored to confirm numerical stability. The solution was considered converged when residuals fell below 1×10^{-5}, ensuring that further iterations produced minimal variations in results.

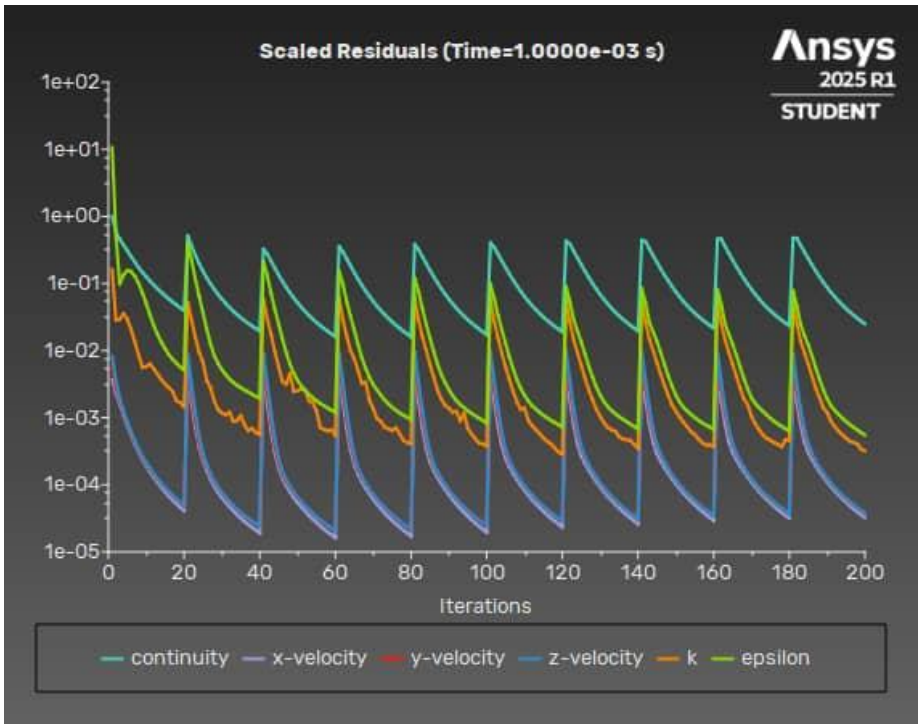

Figure 4.11: Convergence Check

2. Mesh Independence Study: The impact of grid resolution on the accuracy of results was assessed by using different mesh densities:

   i. Coarse Mesh: (~200,000 elements) – Showed significant numerical diffusion and less accurate cavitation predictions.

   ii. Medium Mesh: (~500,000 elements) – Provided reasonable accuracy with balanced computational efficiency.

   iii. Fine Mesh: (~1,000,000+ elements) – Gave highly accurate results but at a higher computational cost.

The mesh independence study confirmed that the chosen grid resolution did not significantly affect the cavitation patterns or pressure distribution, ensuring the reliability of the numerical results.

4.1.3 Literature Validation

To validate the numerical approach, the simulation results were compared with previous studies on cavitation in centrifugal pumps:

i. Comparisons with Water-Based Studies: Existing literature predominantly focuses on water as the working fluid. However, crude oil has a higher viscosity and different vapor pressure properties, requiring modified cavitation models. The results obtained align with general cavitation trends (cavitation inception in the impeller eye) seen in water-based studies shown in figure 4.12 but highlight unique behaviors due to crude oil properties (e.g., slower bubble growth and collapse).

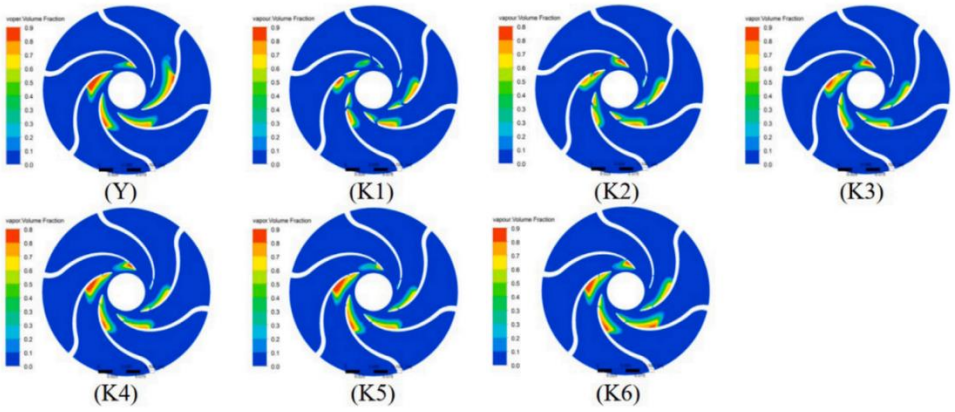

Figure 4.12: CFD result of water cavitation from F. Orlandi et al (2023)

ii. Influence of Surface Roughness: Studies by *Wu et al (2019)* and *Chin Ji. (2019)* confirm that increasing casing roughness intensifies cavitation activity, consistent with the findings from Iteration Two and Three.

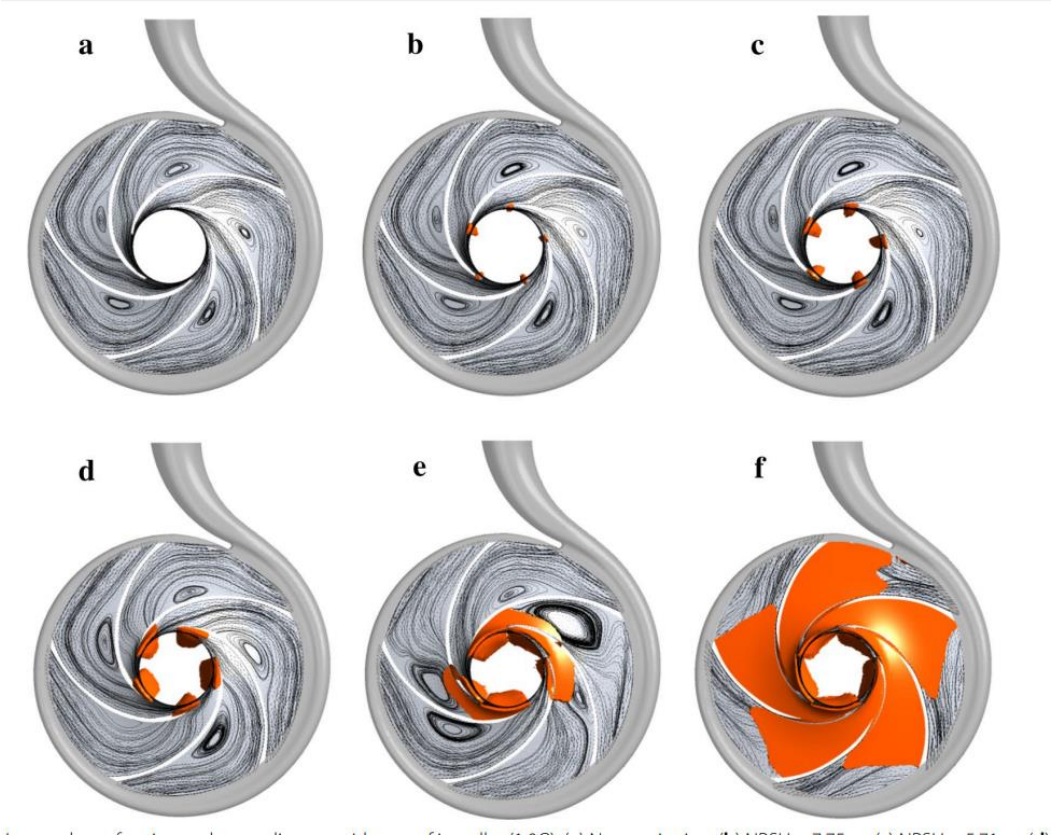

Figure 4.13: CFD result of water cavitation considering wall roughness from Wu et al (2019)

iii. Multiphase and Bubble Dynamics Models: The cavitation patterns predicted using the S-S bubble model, VOF multiphase model, and k-ε turbulence model align with past numerical research, reinforcing the validity of the adopted approach.

4.1.4 Experimental Validation

To further verify the accuracy of the CFD model, the numerical results were compared with actual performance data from an oil rig pump. The experimental validation involved:

i. Pressure Drop Comparison: The simulated pressure drops across the pump stages was found to be within 0.5% margin error of the real-world operational data, confirming the reliability of the CFD predictions.

ii. Cavitation Region Estimation: The CFD model accurately captured cavitation-prone zones that were observed during maintenance inspections of the pump system.

Figure 4.14: Impeller images showing cavitation areas during maintenance

iii. Energy Loss and Efficiency Reduction: The predicted reduction in pump head due to cavitation was consistent with measured values, further supporting the validity of the simulation approach.

CHAPTER 5

CONCLUSION AND RECOMMENDATIONS

5.0 Conclusion

The findings from our transient computational fluid dynamics analysis of crude oil cavitation in centrifugal pumps provide valuable insights into the impact of operating conditions on pump performance and durability. It has been observed that the inception and development of crude oil cavitation are significantly influenced by two primary factors: air backflow and casing roughness. The increase in backflow of air within the pump system promotes vortex formation, leading to an air-lock phenomenon, which disrupts the normal flow of crude oil and intensifies cavitation effects. The presence of entrained air lowers local pressure in specific pump regions, making it more conducive for crude oil to vaporize and form cavitation bubbles. Upon the collapse of these bubbles, high-energy microjets are generated, which erode pump components over time.

Additionally, the increase in casing roughness further contributes to cavitation intensity by promoting flow separation and turbulence, which creates localized pressure drops. The findings highlight that even slight variations in casing surface conditions can escalate cavitation activity, leading to a shorter pump lifespan and reduced operational efficiency.

Contrary to the traditional view that cavitation primarily affects the impeller, this study reveals that its consequences extend to other critical pump components, including bearings and seals. This occurs due to excessive vibrations induced by bubble collapse, which propagates through the pump structure, causing mechanical wear and reducing reliability. Over time, such damage increases maintenance costs, reduces pump efficiency, and leads to unplanned downtime in crude oil transport operations.

Thus, the study emphasizes the necessity of proactive cavitation management strategies, including optimized pump design, effective air management, and surface roughness control. The findings also underline the importance of considering crude oil-specific properties when designing and selecting centrifugal pumps, as conventional water-based cavitation models do not fully capture the complexities observed in crude oil transport.

5.1 Recommendations

Based on the findings from the CFD simulations and cavitation analysis, the following recommendations are proposed to mitigate cavitation effects in crude oil centrifugal pumps and enhance their operational performance:

1. Cavitation Consideration in Pump Design and Selection: Pump manufacturers and oil operators should factor in cavitation resistance when designing or ordering pumps. This includes selecting impeller materials with high cavitation resistance, optimizing impeller geometry to minimize flow separation, and incorporating advanced surface coatings to reduce roughness. Additionally, pump selection should be based on the specific properties of crude oil, ensuring that vapor pressure, viscosity, and density are accounted for in performance assessments.

2. Use of Booster Pumps to Maintain Sufficient Inlet Pressure: One of the most effective strategies to prevent cavitation is ensuring that the inlet pressure remains above the vapor pressure of crude oil. The use of booster pumps before the mainline pump can help achieve this by increasing suction pressure and reducing the risk of vaporization at low-pressure zones. Proper pump staging can significantly reduce cavitation inception, ensuring smoother operation with minimal performance losses.

3. Optimized Operating Conditions for Cavitation Reduction: Pump operators should adhere to operational parameters that balance efficiency and cavitation mitigation. This includes:

    i. Reducing pump speeds where possible to minimize pressure fluctuations.

    ii. Controlling air entrainment by improving sealing mechanisms and suction system design to prevent excessive backflow of air.

    iii. Maintaining an optimal Net Positive Suction Head (NPSH) by ensuring proper suction pipe design, avoiding sharp bends, and preventing obstructions in the flow path.

4. Regular Maintenance and Condition Monitoring: To prevent severe cavitation damage, oil and gas facilities should implement routine inspection schedules for centrifugal pumps. Advanced monitoring techniques, such as vibration analysis, acoustic emission monitoring, and pressure fluctuation tracking, should be employed to detect early signs of cavitation before major damage occurs. Additionally, the use of predictive

maintenance tools powered by AI and machine learning can help operators anticipate cavitation-related failures and schedule proactive interventions.

5. Improved Computational and Experimental Studies for Crude Oil Cavitation: Given the limited research on cavitation in crude oil applications, further studies should be conducted to refine existing models and develop more accurate cavitation prediction tools. Collaboration between academia, industry, and CFD software developers will be essential in improving simulation accuracy, integrating crude oil-specific cavitation parameters, and validating numerical models with real-world experimental data.
6. Implementation of Anti-Cavitation Coatings and Materials: Pump manufacturers should explore wear-resistant coatings and materials that can withstand cavitation-induced erosion. The use of ceramic coatings, composite materials, and hardened alloys in impeller and casing construction can significantly reduce damage caused by bubble collapse, extending the service life of pumps in crude oil applications.
7. Adoption of Alternative Pumping Technologies in Severe Cavitation Environments: In cases where conventional centrifugal pumps experience extreme cavitation, alternative technologies such as positive displacement pumps, magnetic-driven pumps, or hybrid pump designs could be considered. These alternatives offer better performance in handling viscous and cavitation-prone fluids while reducing reliance on impeller-driven flow mechanisms.

REFERENCES

1. Aldi, N., Buratto, C., Pinelli, M., Spina, P. R., Suman, A., & Casari, N. (2016). CFD Analysis of a Non-Newtonian Fluids Processing Pump. Energy Procedia, 101, 742–749. https://doi.org/10.1016/j.egypro.2016.11.094
2. Ali Abdul Mohsin Hassan Nabeel Ahmed Kamal, A., & Abdul Mohsin Hassan, A. (2014). Experimental and Numerical Study on Cavitation Effects in Centrifugal Pumps ، تكهف فقاعة مضخة الرئيسية لكلمات المتوفر لموجب لـ صفي لسحب رفع تجارب فلوت ، Experimental and Numerical Study on Cavitation Effects Nabeel Ahmed Kamal in Centrifugal Pumps. In .Journal of Engineering (Vol. 20)
3. Al-Obaidi, A. R. (2019). Monitoring the performance of centrifugal pump under single-phase and cavitation condition: A CFD analysis of the number of impeller blades. Journal of Applied Fluid Mechanics, 12(2), 445–459. https://doi.org/10.29252/jafm.12.02.29303
4. Ayad, A. F., Abdalla, H. M., & El-Azm Aly, A. A. (2015). Effect of semi-open impeller side clearance on the centrifugal pump performance using CFD. Aerospace Science and Technology, 47, 247–255. https://doi.org/10.1016/j.ast.2015.09.033
5. Baimukhametov, G. F., Kayumov, A. A., Dengaev, A. V., Maksimenko, A. F., Marakov, D. A., Shishulin, V. A., Drozdov, I. M., Samuylova, L. V., Getalov, A. A., Aliev, F. A., & Vakhin, A. V. (2023). Unveiling the Potential of Cavitation Erosion-Induced Heavy Crude Oil Upgrading. Fluids, 8(10). https://doi.org/10.3390/fluids8100274
6. Banerjee, S., Banik, A., Rajak, V. K., Bandyopadhyay, T. K., Nayak, J., Jasinski, M., Kumar, R., Jeon, B. H., Siddiqui, M. R., Khan, M. A., Chakrabortty, S., & Tripathy, S. K. (2024). Two-Phase Crude Oil-Water Flow Through Different Pipes: An Experimental Investigation Coupled with Computational Fluid Dynamics Approach. ACS Omega, 9(10), 11181–11193. https://doi.org/10.1021/acsomega.3c05290
7. Barrios, A. D., Toscano, A. R., & Restrepo, R. R. (2023). CAVITATION PREVENTATION IN CENTRIFUGAL PUMPS USING ANSYS. Journal of Applied Engineering Science, 21(3), 767–777. https://doi.org/10.5937/jaes0-41451
8. Bellary, S. A. I., Husain, A., Samad, A., & Kanai, R. A. (2018). Performance optimization of centrifugal pump for crude oil delivery. Journal of Engineering Research, 15(1), 88–101. https://doi.org/10.24200/tjer.vol15iss1pp88-101
9. Biuok Ehghaghi, M., Amirreza Abdollahi, S., Asri Zamani, K., & Ranjbar, F. (n.d.). Numerical Analysis of Cavitation in a Centrifugal Pump Considering the Impact of Inducer and Fluid Viscosity. https://www.researchgate.net/publication/379257089

10. Boitel, G., Fedala, D., & Myon, N. (2016). Tip clearance effects on loads and performances of semi-open impeller centrifugal pumps at different specific speeds. IOP Conference Series: Earth and Environmental Science, 49(3). https://doi.org/10.1088/1755-1315/49/3/032013
11. Dong, J., & Li, W. (2023). Numerical Simulation of Centrifugal Pump Cavitation Based on ANSYS. Journal of Physics: Conference Series, 2450(1). https://doi.org/10.1088/1742-6596/2450/1/012031
12. Huang, S., Hu, Y., Wei, Y., & Mo, Y. (2023). Analysis of Cavitation Flow Performance in Centrifugal Pump Using OpenFOAM. Journal of Physics: Conference Series, 2610(1). https://doi.org/10.1088/1742-6596/2610/1/012023
13. Hussein, A. (2023). Chapter 2 - Flow Assurance. In A. Hussein (Ed.), Essentials of Flow Assurance Solids in Oil and Gas Operations (pp. 53–103). Gulf Professional Publishing. https://doi.org/https://doi.org/10.1016/B978-0-323-99118-6.00015-0
14. Khan, Z., & Weiguo, Z. (2024). Cavitation mitigation via curvilinear barriers in centrifugal pump. Discover Mechanical Engineering, 3(1). https://doi.org/10.1007/s44245-024-00045-8
15. Kozubková, M., Rautová, J., & Bojko, M. (2012). Mathematical model of cavitation and modelling of fluid flow in cone. Procedia Engineering, 39, 9–18. https://doi.org/10.1016/j.proeng.2012.07.002
16. Li, C., He, J., Jia, W., Yang, F., Ban, J., & Qiu, B. (2023a). Modeling transient cavitating flow in large drop crude oil pipelines. Journal of Petroleum Science and Engineering, 220. https://doi.org/10.1016/j.petrol.2022.111241
17. Li, G., Sun, H., He, J., Ding, X., Zhu, W., Qin, C., Zhang, X., Zhou, X., Yang, B., & Guo, Y. (2024). Deep learning, numerical, and experimental methods to reveal hydrodynamics performance and cavitation development in centrifugal pump. Expert Systems with Applications, 237. https://doi.org/10.1016/j.eswa.2023.121604
18. Liu, Q., Qi, X., Zhu, Z., Gao, Y., Yang, G., Li, C., & Sun, L. (2024). Investigation of cavitation characteristics in an aircraft centrifugal fuel pump. Flow Measurement and Instrumentation, 96. https://doi.org/10.1016/j.flowmeasinst.2024.102521
19. Luo, H., Wen, J., Lv, C., & Wang, Z. (2022a). Modeling of viscosity of unstable crude oil–water mixture by characterization of energy consumption and crude oil physical properties. Journal of Petroleum Science and Engineering, 212. https://doi.org/10.1016/j.petrol.2022.110222

20. Mousmoulis, G., Karlsen-Davies, N., Aggidis, G., Anagnostopoulos, J., & Papantonis, D. (2017a). Experimental analysis of the onset and development of cavitation in a centrifugal pump. Journal of Physics: Conference Series, 813(1). https://doi.org/10.1088/1742-6596/813/1/012044
21. Mousmoulis, G., Kassanos, I., Aggidis, G., & Anagnostopoulos, I. (2021). Numerical simulation of the performance of a centrifugal pump with a semi-open impeller under normal and cavitating conditions. Applied Mathematical Modelling, 89, 1814–1834. https://doi.org/10.1016/j.apm.2020.08.074
22. Orlandi, F., Montorsi, L., & Milani, M. (2023a). Cavitation analysis through CFD in industrial pumps: A review. In International Journal of Thermofluids (Vol. 20). Elsevier B.V. https://doi.org/10.1016/j.ijft.2023.100506
23. Ravikumar, V. (2023). Pumps. In Sprinkler and Drip Irrigation (pp. 597–639). Springer Nature Singapore. https://doi.org/10.1007/978-981-19-2775-1_23
24. Shinde, P., & Satam, A. (2014). Cavitation Effect in Centrifugal Pump. International Journal of Researchers, Scientists and Developers, 2(2). www.ijrsd.org
25. Wang, J., Sun, L., Zhou, Y., Liu, Y., & Zhao, F. (2023). Numerical Simulation of Cavitation Characteristics of a Centrifugal Pump Based on an Improved ZGB Model. Processes, 11(2). https://doi.org/10.3390/pr11020438
26. Wasswa, D. (n.d.). OF THE THEORY OF FLUID FLOW FIFTH EDITION. https://www.researchgate.net/publication/364642982
27. Wilcox, D. C. . (2010). Turbulence modeling for CFD. DCW Industries.
28. Wu, D., Ren, Y., Mou, J., Gu, Y., & Jiang, L. (2019). Unsteady Flow and Structural Behaviors of Centrifugal Pump under Cavitation Conditions. Chinese Journal of Mechanical Engineering (English Edition), 32(1). https://doi.org/10.1186/s10033-019-0328-8
29. Xie, H., Luo, X. Q., Feng, J. J., Zhu, G. J., & Li, C. H. (2024). Application of three cavitation models in centrifugal pump cavitation flow simulation. Journal of Physics: Conference Series, 2707(1). https://doi.org/10.1088/1742-6596/2707/1/012141
30. Zhang, Z. Y., & Luo, X. W. (2024). Numerical investigation on cavitation performance for centrifugal pumps with different impeller inlet geometry. Journal of Physics: Conference Series, 2707(1). https://doi.org/10.1088/1742-6596/2707/1/012045